

Review #1

This is a well-written manuscript covering the cycling of cobalt in the Arctic Ocean. The cobalt measurements in the manuscript are high quality. The use of the Tagliabue's biogeochemical model with the addition of cobalt with the PISCES-v2 module provides insight into the likely sources of cobalt to the Arctic water column. I have not substantive comments on the manuscript.

Some minor comments -

line 269: the GitHub link doesn't contain any information

Thank you, this has been fixed.

lines 369 to 375: this information is also presented in table 1 so it is repetitive - I suggest it is removed from here and just refer to the Table.

We have now shortened this section and combined it with the following section.

line 1060: Saito et al. 2001 reference is cited twice.

Thank you, this has now been fixed.

Review #2

This is an important, well written manuscript. I think it should be published in Bio- geosciences, however I have a number of comments that should be addressed first. My comments are listed in the order I came across them in the manuscript, not by importance.

Line 2: Has Co actually every been shown to limit phytoplankton growth in the ocean? Certainly not in many regions? Suggest to modify phrasing accordingly.

We clarified this statement to refer to cobalt's role as a co-factor in cyanocobalamin, which has been shown to limit phytoplankton growth in several regions of the oceans. Cobalt has also been shown to be serially limiting with nitrogen and iron (Browning et al., 2017). We updated this sentence to read, "Cobalt (Co) is an important bioactive trace metal that is the metal co-factor in cobalamin (vitamin B₁₂) which can limit or co-limit phytoplankton growth in many regions of the ocean."

Line 40: Again, might be misleading to state that Co has been found to be the growth limiting nutrient?

We amended this section to read, "Due to its low concentrations, strong organic complexation, and its presence in cobalamin, dCo or cobalamin have been found to be limiting or co-limiting nutrients for phytoplankton growth in several regions (Bertrand et al., 2007, 2015; Browning et al., 2017; Martin et al., 1989; Moore et al., 2013; Saito et al., 2005). Growth limitation can be due to either a lack of dCo, or cobalamin (Bertrand et al., 2012; Bertrand et al., 2007; Browning et al., 2017), as cobalamin is only synthesized by cyanobacteria and some archaea (Doxey et al., 2015). However, many phytoplankton utilize cobalamin for the synthesis of methionine (Yee and Morel, 1996; Zhang et al., 2009), and therefore must obtain it from the natural environment (Heal et al., 2017)."

Line 130: "pressurized filtered air" – N₂ gas?

Correct, the samples were collected using filtered pressurized air and not N₂ gas.

Line 131: States collection methods for Co, then nutrients, and then back to Co again. Move nutrient sampling to end of paragraph?

We have now moved the nutrient methods information to the end of the paragraph.

Section 2.2: Not clear if samples for Co were acidified for storage or not?

Samples were not acidified. We clarified this in Section 2.2: "...samples were kept refrigerated (4 °C) and un-acidified until analysis (Hawco et al., 2016, 2018; Noble et al., 2016). LCo samples were double-bagged and stored at 4 °C and un-acidified until analysis."

Section 2.8:

- Briefly comment here on how PISCES-v2 performs in terms of physics/ice/rivers/macronutrients/chlorophyll in the Arctic Ocean, as these are key for interpreting the results.

The PISCES model has been used extensively to examine global scale biogeochemical cycling. We did not choose here to make an extensive model evaluation study in the Arctic Ocean since this was not the focus of the paper. Instead, the goal was to explore how the model's cobalt sources, sinks and internal cycling performed and how they may help provide additional insight into the driving mechanisms behind the observed distributions. Thus we chose to focus the model evaluation on cobalt rather than a suite of extra tracers that would lengthen the manuscript and distract from its focus. More details on PISCES can be found in the cited reference publications (Aumont et al., 2015; 2017; Tagliabue et al., 2018).

- Please state whether Co concentrations regulate phytoplankton growth in the model.

Co concentrations do not regulate phytoplankton growth in the model. Uptake of Co by phytoplankton in the model is explicitly modeled based on a maximum cellular quota and allows for variable Co/C ratios (Tagliabue et al., 2018).

- Please indicate whether there are Co binding ligands in the model, what their sources are etc. (as DOM complexation of dCo is inferred as important mechanism protecting against scavenging in the observational data, and could be an important factor contributing to differences with the model)

Organic cobalt-binding ligands are modeled and are linked to the relative abundance of nanoplankton in the model as a means of representing the production of cobalamin or pseudocobalamin by picocyanobacteria communities. Co ligands also have a minimum deep ocean concentration in the model to stabilize dCo in the deep ocean and prevent scavenging. A few additional details about the model have been added to the manuscript in section 2.8 based on the suggestions above. Extensive details can be found in Tagliabue et al. (2018).

Lines 355–359: Repetition of how PHW can be identified?

We have shortened this to read, “The PHW can be clearly identified from the elevated macronutrient concentrations (Fig. 2D), and temperature maximum within the salinity range of 31–33 (Steele et al., 2004; Steele and Boyd, 1998) (Fig. 2A, C).”

Line 513–516: Perhaps rephrase to make clear that it is dissolution of Mn-oxides with Co bound to it is a Co source (not the Mn-oxide itself).

We have clarified this and rephrased.

Section 3.5: There is a lot of discussion in this results section. The discussion including comparison to other regions and hypothesized mechanisms controlling Co distributions should be moved to the discussion section.

We removed several lines of text from this section and combined it with the text in the second paragraph of section 4.1 of the discussion.

Line 553: Insert ‘as indicated by dMn concentrations’ when refereeing to shelf inputs?

This has been inserted.

Line 557: Replace ‘diminished’ by ‘low’ (i.e. diminished relative to what?)

This has been changed to indicate that there is diminished scavenging of dCo in the model relative to other ocean basins (Tagliabue et al., 2018).

Line 559: Which transect is being referred to here?

This has been changed to specify the GN01 transect.

Lines 620–623: Sentence unclear – please rephrase

This has been changed to read, “The interaction between rivers and shelves requires further study, as the shelf sediments might behave as “capacitor” for dCo, accumulating Co from rivers and sinking organic matter and then releasing Co to the overlying water during reductive dissolution in the sediments. Although the mechanism is uncertain, it is clear that the riverine source dominates the distribution observed near the North Pole where dCo and LCo concentrations remain high despite the distance from land, and that organic complexation likely plays a role in the distal transport of this dCo (Charette et al., 2020).”

Line 679: Rephrase to state that it is a combination of restricted upper ocean scavenging in combination with continued deep water scavenging alongside restricted water mass mixing? i.e. Need to keep clear that there is expected lower scavenging in surface waters as these are argued to be important for leading to the high dCo there? If this is not what the author’s intended to say then this bit needs a little rephrasing.

This section has been amended as follows:

“This evidence, combined with the coinciding maxima observed in pCo and pMn, suggest that scavenging occurs in the upper water column, but that additional scavenging continues to occur in deeper waters. The elevated pCo concentrations in the deep Arctic compared to other regions (Lee et al., 2018) suggest that scavenging over long timescales continues to add to the pCo pool. The strong stratification in the Arctic likely prevents high concentrations of dCo from mixing between the modified surface waters, the PHW, and the deep Atlantic water (Steele et al., 2004). Thus, it is likely a combination of limited upper ocean scavenging, and strong stratification between water masses, that keeps the elevated dCo and LCo confined to the surface waters in Arctic, yielding the intense scavenged-like profile of Co in this region compared to other basins (Fig. 3).”

Line 706: Rephrase to state that it is the observed increase in dCo over two time points. i.e., seasonal or inter-annual variability could explain this.

We have updated this sentence to read, “While there is not enough data to state whether the river dCo flux has in fact changed over time in the Arctic and the observed changes could be due to seasonal or interannual variability, several other studies have documented an increase in river discharge due to increases in permafrost melt over time (Doxaran et al., 2015; Drake et al., 2018; Kipp et al., 2018; van der Loeff et al., 2018; Tank et al., 2016; Toohey et al., 2016).”

Paragraph starting line 736: Can this not be investigated with the PISCES model output? If the model is doing a good job in replicating Co in the Arctic for the correct mechanisms, then would export into the Atlantic Ocean not be replicated by the model? If so then the authors can be a bit more quantitative about this statement (e.g. providing an approximate fraction of Arctic-sourced Co in the Atlantic). If the model is not replicating this, then this would still be interesting to comment upon (i.e. either the model or the proposed mechanism is incorrect).

The downstream impact of the Arctic on the Atlantic Co distribution can be seen in the results of Tagliabue et al. 2018, but were not focused on in that paper. The clearest way to quantify the influence of the Arctic on the North Atlantic dCo distribution would be to “turn off” the Arctic sources of dCo in the model and see how that impacts distributions in the North Atlantic. However, this is not straightforward and fully masking all of the sources of Co in the Arctic is currently not possible in the current model framework. Alternative tests, such as picking experiments that led to strong reductions in Arctic Co levels (e.g. the experiments where bacterial activity did not affect the Co scavenging rate from Tagliabue et al, 2018) are also not ideal as the Arctic signal itself is not isolated.

We also felt we were not able to be quantitative about the Co source to the North Atlantic from observations alone because the transformations and source regions of Labrador Sea water are not entirely understood at this time (Le Bras et al., 2017), so it is difficult to say with the current data what proportional of the high dCo signal seen in Noble et al. (2016) is due to additional dCo sources on the western margin of the US.

Line 799: Again the authors should stress here that this is just two time points of observations and therefore not enough data to say whether Co concentrations in the Arctic are increasing with time.

We amended this section to make sure it is clear that the dataset is limited. It now reads, “Co was also shown in this work to be increasing over time on the shelf in the Canadian Arctic, possibly due to increases in river inputs from thawing permafrost, though this is difficult to constrain in the present limited dataset. Given the potential increase in Co over time in the Arctic and the modification of low-salinity Arctic waters as they exit the Arctic into the North Atlantic and the Labrador Sea, it is difficult to determine if there is a net flux of Co out of the Arctic and into the North Atlantic, however evidence in this work suggests that the distinct Co waters of the Arctic likely impact downstream micronutrient concentrations. These impacts are likely to become increasingly important in the future, with increased warming and changes to Co sources in the Arctic basin.”

Figures 8 and 9: Possible to make the colour bar numbers larger?

Yes, we made the labels on Figures 8-10 larger.

References

Bertrand, E. M., Saito, M. A., Rose, J. M., Riesselman, C. R., Lohan, M. C., Noble, A. E., Lee, P. A. and DiTullio, G. R.: Vitamin B₁₂ and iron colimitation of phytoplankton growth in the Ross Sea, *Limnol. Oceanogr.*, 52(3), 1079–1093, doi:10.4319/lo.2007.52.3.1079, 2007.

Bertrand, E. M., Allen, A. E., Dupont, C. L., Norden-Krichmar, T. M., Bai, J., Valas, R. E. and Saito, M. A.: Influence of cobalamin scarcity on diatom molecular physiology and identification of a cobalamin acquisition protein, *Proc. Natl. Acad. Sci.*, 109(26), E1762–E1771, doi:10.1073/pnas.1201731109, 2012.

Bertrand, E. M., McCrow, J. P., Moustafa, A., Zheng, H., McQuaid, J. B., Delmont, T. O., Post, A. F., Sipler, R. E., Spackeen, J. L. and Xu, K.: Phytoplankton–bacterial interactions mediate micronutrient colimitation at the coastal Antarctic sea ice edge, *Proc. Natl. Acad. Sci.*, 112(32), 9938–9943, 2015.

Browning, T. J., Achterberg, E. P., Rapp, I., Engel, A., Bertrand, E. M., Tagliabue, A. and Moore, C. M.: Nutrient co-limitation at the boundary of an oceanic gyre, *Nature*, 551(7679), 242–246, doi:10.1038/nature24063, 2017.

Charette, M. A., Kipp, L. E., Jensen, L. T., Dabrowski, J. S., Whitmore, L. M., Fitzsimmons, J. N., Williford, T., Ulfssbo, A., Jones, E., Bundy, R. M. and others: The Transpolar Drift as a Source of Riverine and Shelf-Derived Trace Elements to the Central Arctic Ocean, *J. Geophys. Res. Ocean.*, 2020.

Doxaran, D., Devred, E. and Babin, M.: A 50% increase in the mass of terrestrial particles delivered by the Mackenzie River into the Beaufort Sea (Canadian Arctic Ocean) over the last 10 years, 2015.

Doxey, A. C., Kurtz, D. A., Lynch, M. D. J., Sauder, L. A. and Neufeld, J. D.: Aquatic metagenomes implicate Thaumarchaeota in global cobalamin production, *ISME J.*, 9(2), 461, 2015.

Drake, T. W., Tank, S. E., Zhulidov, A. V., Holmes, R. M., Gurtovaya, T. and Spencer, R. G. M.: Increasing alkalinity export from large Russian Arctic rivers, *Environ. Sci. Technol.*, 52(15), 8302–8308, 2018.

Hawco, N. J., Ohnemus, D. C., Resing, J. A., Twining, B. S. and Saito, M. A.: A dissolved cobalt plume in the oxygen minimum zone of the eastern tropical South Pacific, *Biogeosciences*, 13(20), 5697–5717, doi:10.5194/bg-13-5697-2016, 2016.

Hawco, N. J., Lam, P. J., Lee, J. M., Ohnemus, D. C., Noble, A. E., Wyatt, N. J., Lohan, M. C. and Saito, M. A.: Cobalt scavenging in the mesopelagic ocean and its influence on global mass

balance: Synthesizing water column and sedimentary fluxes, *Mar. Chem.*, 201(March 2017), 151–166, doi:10.1016/j.marchem.2017.09.001, 2018.

Heal, K. R., Qin, W., Ribalet, F., Bertagnolli, A. D., Coyote-Maestas, W., Hmelo, L. R., Moffett, J. W., Devol, A. H., Armbrust, E. V. and Stahl, D. A.: Two distinct pools of B12 analogs reveal community interdependencies in the ocean, *Proc. Natl. Acad. Sci.*, 114(2), 364–369, 2017.

Kipp, L. E., Charette, M. A., Moore, W. S., Henderson, P. B. and Rigor, I. G.: Increased fluxes of shelf-derived materials to the central Arctic Ocean, *Sci. Adv.*, 4(1), eaao1302, 2018.

Lee, J.-M., Heller, M. I. and Lam, P. J.: Size distribution of particulate trace elements in the US GEOTRACES Eastern Pacific Zonal Transect (GP16), *Mar. Chem.*, 201, 108–123, 2018.

Le Bras, I. A., Yashayaev, I. and Toole, J. M.: Tracking Labrador Sea water property signals along the deep western boundary current, *J. Geophys. Res. Ocean.*, 122(7), 5348–5366, 2017.

Martin, J. H., Gordon, R. M., Fitzwater, S. and Broenkow, W. W.: VERTEX: phytoplankton/iron studies in the Gulf of Alaska, *Deep Sea Res. Part A. Oceanogr. Res. Pap.*, 36(5), 649–680, 1989.

Moore, C. M., Mills, M. M., Arrigo, K. R., Berman-Frank, I., Bopp, L., Boyd, P. W., Galbraith, E. D., Geider, R. J., Guieu, C., Jaccard, S. L., Jickells, T. D., La Roche, J., Lenton, T. M.,

Mahowald, N. M., Marañón, E., Marinov, I., Moore, J. K., Nakatsuka, T., Oschlies, A., Saito, M. A., Thingstad, T. F., Tsuda, A., Ulloa, O., Marañon, E., Marinov, I., Moore, J. K., Nakatsuka, T., Oschlies, A., Saito, M. A., Thingstad, T. F., Tsuda, A. and Ulloa, O.: Processes and patterns of oceanic nutrient limitation, *Nat. Geosci.*, 6(9), 701–710, doi:10.1038/ngeo1765, 2013.

Noble, A. E., Ohnemus, D. C., Hawco, N. J., Lam, P. J. and Saito, M. A.: Coastal sources, sinks and strong organic complexation of dissolved cobalt within the US North Atlantic GEOTRACES transect GA03, *Biogeosciences*, 14(11), 2715–2739, doi:10.5194/bg-14-2715-2017, 2016.

Saito, M. A., Rocap, G. and Moffett, J. W.: Production of cobalt binding ligands in a *Synechococcus* feature at the Costa Rica upwelling dome, *Limnol. Oceanogr.*, 50(1), 279–290, 2005.

Saito, M. A., Goepfert, T. J., Noble, A. E., Bertrand, E. M., Sedwick, P. N. and DiTullio, G. R.: A seasonal study of dissolved cobalt in the Ross Sea, Antarctica: micronutrient behavior, absence of scavenging, and relationships with Zn, Cd, and P, *Biogeosciences*, 7(12), 4059–4082, doi:10.5194/bg-7-4059-2010, 2010.

Steele, M. and Boyd, T.: Retreat of the cold halocline layer in the Arctic Ocean, *J. Geophys. Res. Ocean.*, 103(C5), 10419–10435, 1998.

Steele, M., Morison, J., Ermold, W., Rigor, I., Ortmeier, M. and Shimada, K.: Circulation of summer Pacific halocline water in the Arctic Ocean, *J. Geophys. Res. Ocean.*, 109(C2), 2004.

Tagliabue, A., Hawco, N. J. N. J., Bundy, R. M. R. M., Landing, W. M. W. M., Milne, A.,

Morton, P. L. P. L. and Saito, M. A. M. A.: The role of external inputs and internal cycling in shaping the global ocean cobalt distribution: insights from the first cobalt biogeochemical model, *Global Biogeochem. Cycles*, 32(4), 1–23, doi:10.1002/2017GB005830, 2018.

Tank, S. E., Striegl, R. G., McClelland, J. W. and Kokelj, S. V: Multi-decadal increases in dissolved organic carbon and alkalinity flux from the Mackenzie drainage basin to the Arctic Ocean, *Environ. Res. Lett.*, 11(5), 54015, 2016.

Toohey, R. C., Herman-Mercer, N. M., Schuster, P. F., Mutter, E. A. and Koch, J. C.: Multidecadal increases in the Yukon River Basin of chemical fluxes as indicators of changing flowpaths, groundwater, and permafrost, *Geophys. Res. Lett.*, 43(23), 12–120, 2016.

van der Loeff, M., Kipp, L., Charette, M. A., Moore, W. S., Black, E., Stimac, I., Charkin, A., Bauch, D., Valk, O., Karcher, M. and others: Radium isotopes across the Arctic Ocean show time scales of water mass ventilation and increasing shelf inputs, *J. Geophys. Res. Ocean.*, 123(7), 4853–4873, 2018.

Yee, D. and Morel, F. M. M.: In vivo substitution of zinc by cobalt in carbonic anhydrase of a marine diatom, *Limnol. Oceanogr.*, 41(3), 573–577, 1996.

Zhang, Y., Rodionov, D. A., Gelfand, M. S. and Gladyshev, V. N.: Comparative genomic analyses of nickel, cobalt and vitamin B12 utilization, *BMC Genomics*, 10(1), 78, 2009.

Review #3

Review of 'Elevated sources of cobalt in the Arctic Ocean' by Bundy et al.

The authors present novel data from an understudied region. The data appears of high quality, is definitely very interesting and as such should be published. Generally the paper is well written, but the methods and results section seem quite long. I like that the methods are detailed, but given that most methods have been described before I wonder if all details are required here and if the methods section could be condensed. The results section already contains quite some discussion. This should either be moved to the discussion, or perhaps a combined results/discussion section is more suitable for this paper (i.e. where the actual results section only briefly describes the basin wide distribution). The number of figures is also quite large and I encourage the authors to reconsider if they need them all as the sheer volume of data presented is a bit overwhelming.

Thank you for the comments. We have shortened the methods section where possible, and have moved some sentences from the results section to the discussion, particularly from the modeling results section (section 3.5). We realize the volume of data and the numbers of figures is quite large, however for completeness we have kept all of the figures and tables.

Generally, the discussion is interesting, but I thought it was strange that work already published from this cruise (e.g. Jensen et al., 2019) or the German/Dutch GEOTRACES cruises (both 2015 and 2007 GEOTRACES IPY) is barely (or not at all) discussed. There is already quite some work that provides very nice context for the current study, e.g. the work on Fe and Fe binding ligands in the TPD from the GN04 transect, the Jensen Zn study or the Mn and Fe work from the GIPY 11 cruise (data in IDP). The same can be said for the comparison with the Atlantic where the comparison is made with data quite far south along the zonal GA03 rather than the also available meridional GA02 data that seems more relevant for the discussion of advection into the Atlantic.

As discussed in the specific comments below, we have added many of these references throughout the discussion section. We have kept our current comparison to GA03, but we have mentioned that a similar signal was observed in GA02 in LSW.

In the section on correlations, mixing as a driving factor in such correlations is ignored (see also specific comments) and this is something that in my opinion should be addressed. The comparison with the data from 2009 is definitely interesting, but way overstated. Most importantly, 2 data points in time are not proof of a trend. Moreover, there could be seasonal variation (as it appears the stations were not occupied at the same time/season) and the stations locations are actually quite far apart. Notably the width (area) of the adjacent/closest shelf is very different and stations were positioned differently with respect to fluvial input and the Bering Strait. In this study it is argued that the shelf is the most important source of Co. Thus higher concentrations in the vicinity of the large shelf area of the Chukchi Sea and Bering Strait compared to the narrow Canada basin shelf are maybe not that surprising and this needs to be

explored in context of the local hydrography and currents. I also noted (based on Fig 9) that the role that bacteria play differs between the regions for the 2009 and 2015 data.

We discussed some of these suggestions below in the specific comments. We believe that the stratification in the Arctic basin which impedes mixing between the Pacific waters and Atlantic waters as shown in this work (and others), would suggest that the impact of mixing of water masses on the Co:P stoichiometry observed is minimal. The water masses in this region have very little exchange (Figure 2) and thus the primary drivers of changes in the deep Co:P ratios are likely due to internal cycling.

We have also noted this extensively below, but we did not intend to suggest that our dCo from 2009 and 2015 is definitive evidence that Co is increasing over time in the Arctic, as we discussed many caveats in the manuscript. However, we do feel it is an important observation to document in our work.

The conclusions were not completely appropriate for the current ms. The data/ms did not show at all that the Co distribution has implications for Arctic ecosystems and it is unclear how the observation of a unique Co distribution affects future changes in micro nutrients. As stated above, I do not believe that Co was shown in this work to be increasing over time. The idea that (changing) conditions in the Arctic affect the North Atlantic Ocean downstream is not new and this should be acknowledged.

We have reworked section 4.3 and 4.4 of the discussion to make it clearer that we were not trying to say that our data shows that dCo has unequivocally been increasing over time in the Arctic. We have pointed out that our data suggests that dCo is increasing, however we recognize that the data is limited. However, since others have noted the same trend in other tracers, we do not believe our conclusions are unjustified. We have cited several papers that have also noted increases in shelf-derived tracers in the Arctic over time and their effects to the downstream North Atlantic (Charette et al., 2020; Kipp et al., 2018; van der Loeff et al., 2018).

Specific comments 40-43 limitation by cobalamin does not necessarily imply Co limitation as cobalamin production can be low regardless of the Co levels. So most of the cited studies do not demonstrate Co limitation.

We clarified this sentence to read, “Due to its low concentrations, strong organic complexation, and its presence in cobalamin, dCo or cobalamin have been found to be limiting or co-limiting nutrients for phytoplankton growth in several regions (Bertrand et al., 2007, 2015; Browning et al., 2017; Martin et al., 1989; Moore et al., 2013; Saito et al., 2005). Growth limitation can be due to either a lack of dCo, or cobalamin (Bertrand et al., 2012; Bertrand et al., 2007; Browning et al., 2017), as cobalamin is only synthesized by cyanobacteria and some archaea (Doxey et al., 2015).”

76-80 it is stated there are regionally specific features, but the examples are not really specific regional features. Perhaps rephrase?

This sentence was removed.

92 awkward sentence, please rephrase

This has been rephrased as “This study examined dCo, LCo, and pCo in two different transects in the Canadian sector of the Arctic Ocean.”

94 what is meant with ‘interpreting the role of external sources and internal cycling to the distribution’?

We meant that we used the model to evaluate our hypotheses about the key factors in controlling dCo distributions in the Arctic. We changed this sentence to, “We then used a Co biogeochemical model (Tagliabue et al., 2018) in order to evaluate hypotheses about the role of external sources and internal cycling to the observed Co distributions, the potential of the Arctic to be a net source of Co to the North Atlantic, and to identify Co sources and sinks that may be sensitive to future changes in this rapidly changing ocean basin.”

109 was sampled

We left this sentence as is.

131 can you compare filtered and unfiltered samples? Perhaps state this will be addressed later in the ms

This was addressed later in the manuscript.

295 this detection limit is at least an order of magnitude too high for open ocean Mn, notably in the deep. Is it a typo?

This is not a typo, and refers to the detection limit of shipboard flow injection analyses of dMn and not ICP-MS analyses.

324 Fe was already defined

Thank you, this has been fixed.

389 given that the data from the Canadian geotraces cruise was unfiltered, I do not think it is appropriate to call it dissolved (dCo)

This section is about the GN01 data, which are all filtered.

408 how is the % sea ice melt determined?

This is determined from $\delta^{18}O$ data (Newton et al., 2013). This reference has been added.

427 what is the % Pacific water based on?

Same as above.

427 here and elsewhere, the number of significant figures for Co concentrations does not seem to match the reported precision.

All data presented have the correct number of significant figures.

470 awkward sentence, please rephrase

This has been rephrased.

471 what does 'that' refer too?

This has been rephrased to, "Similar to dCo, there was no observable enhancement of LCo in PHW, with LCo distributions closely following that of dCo and other shelf-enhanced trace metals such as dFe and dMn."

508 confused, 'capture the major processes contributing to modeled sources and sinks' not sure what is meant here.

This has been amended to, "In order to explore the major processes contributing to the modeled dCo sources and sinks, the proportion of the dCo signal in two distinct depth horizons was further investigated using a set of sensitivity experiments."

516-517 Jensen et al 2019 argued that low oxygen in the sediments plays an important role for Zn and evidence for denitrification in the sediments was presented. This should also affect Co despite the fact that oxygen is not low in the water column. If denitrification occurs in the sediments, isn't it likely that also reductive dissolution of sedimentary Mn-oxides occurs? (however this discussion seems out of place in the results section)

Yes, it is possible that there may be denitrification occurring in the sediments which could impact the dMn and dCo distributions. This is accounted for indirectly in the model by the sediment Co source being a function of the particulate organic carbon (POC) flux, which is a primary driver of anoxic sediments and thus denitrification.

516-534 this section is not as clearly written as the rest of the ms (specifically the last sentence was impossible to follow for me). Perhaps this can be remedied?

We have re-worded several sentences in this section.

540-554 There is a problem with this section as for the Arctic (but also elsewhere, e.g. Aguilar-Islas A. and Bruland K. W. (2006)) it has been demonstrated that Mn in the surface of the open ocean basin is mainly derived from fluvial input, not sediments (Middag et al., 2011 (doi:10.1016/j.gca.2011.02.011)). The latter study was not the exact same region, but fluvial input will be a strong source of Mn in this region too, and this needs to be discussed. However, Zn (Jensen et al., 2019) has been shown to have an important sedimentary source and might be a better proxy?

Middag et al. (2011) and Charette et al. (2020) both suggest that dMn in the Arctic has both a fluvial and sedimentary source. In the Arctic, it is difficult to disentangle the shelf and riverine processes, as the riverine inputs interact with the shelf before being transported to the open basins (Kipp et al. 2018). The same is true for the dCo, which we mention in section 4.1. We have amended this section to highlight that although we believe the shelf signal to be the primary dCo source, we note that the fluvial inputs are very important in the open basin due to the TPD.

571 discussion of the recent TPD paper here seems appropriate as well as some recent Fe work

Yes, these references have now been updated since the recent publication of Charette et al. (2020), Colombo et al., (2020) and Tonnard et al. (2020).

572/573 ‘track shelf inputs due to interactions between the sediment-water exchange processes’ quite vague, not sure what this means/implies

We have clarified this sentence to indicate that radium is a tracer for shelf inputs.

582-584 What about deposition of riverine Co in the shelf sediments and subsequent remobilization?

Yes, this could be another process on the shelf that is contributes to elevated dCo and is mentioned later on in this section.

590 also argued for Fe (<https://doi.org/10.1016/j.marchem.2017.10.005>; <https://doi.org/10.1029/2018JC014576>)

We have added these references.

597 see mentioned refs for humic-like substances and Fe in the TPD, seems very relevant here.

Yes, these have been added.

662 what is meant with depth here? I assume the slopes are determined per station and the depth is the station depth or am I wrong? Please clarify

We have reworded this to be “versus depth.”

654-670 there is a growing body of work demonstrating mixing and water mass circulation is a primary factor in driving the slopes of metal-nutrient relationships that is ignored here while the mixing of Pacific and Atlantic origin water could have a strong effect (e.g. Vance et al., 2017, doi: 10.1038/ngeo2890; de Souza et al., 2018, doi:10.1016/j.epsl.2018.03.050; Middag et al., 2018, doi: 10.1016/j.epsl.2018.03.046; Weber et al., 2018, doi: 10.1126/science.aap8532; Middag et al., 2019, doi:10.1029/2018GB006034; Middag et al., 2020 doi: 10.3389/fmars.2020.00105).

This is very important to consider in other ocean basins, but there is very little mixing in the Arctic between water masses due to the strong stratification, so we do not think this is significant

here. This is also likely not as important for dCo, which has a much shorter residence time (~200 years) compared to some of the longer residence time elements mentioned in these references.

676 continues?

This has been changed.

702 after a 40% correction, the 2015 data is 400% higher than the 2009 data. This seems to be in contrast to line 688 where it is stated that without correction the 2015 data is 3.5 times higher.

This has been corrected.

703-704 could there be a factor of seasonality (did the sampling occur in same time of year relative to start of ice melt and river discharge)? And 2 data points in time hardly makes a trend! The difference is interesting for sure, but currently the significance is really overstated, as there is no way of telling what the Co concentrations were in other years. What about the enormous difference in the size of the nearby shelf regions between the 2 expeditions?

Yes, both samplings were done in the same month of the year (October). We have discussed many of these points extensively in this section, and have been transparent about the caveats. Many others have also observed increases in fluvial and shelf tracers over time in the Arctic however (Doxaran et al., 2015; Drake et al., 2018; Kipp et al., 2018; van der Loeff et al., 2018; Tank et al., 2016; Toohey et al., 2016), so we do believe that our data could be pointing to an increase in dCo over time as well. We have thoroughly explained these caveats in this section.

“The increase in dCo over time in the Arctic is interesting, and has been documented for other tracers in the Arctic. Kipp et al. (2018) and van der Loeff et al. (2018) noted that ^{228}Ra has increased over time in the central Arctic. They suggest that increases in shelf and/or river inputs from thawing permafrost are the source of this elevated ^{228}Ra (Kipp et al., 2018; van der Loeff et al., 2018). The increase in metal inventories over time on Arctic shelves is consistent with this observation. The majority of the variance (~70%) in dCo in the upper 100 m on the U.S. GEOTRACES transect could be explained by a shelf source, and the remainder was likely associated with river inputs (Fig. 11). If these sources are similar to the sources of dCo in 2009, then an increase in either a shelf or river flux could be responsible for the dramatic increase in dCo over time. While there is not enough data to state whether the river dCo flux has in fact changed over time in the Arctic and the observed changes could be due to seasonal or interannual variability, several other studies have documented an increase in river discharge due to increases in permafrost melt over time (Doxaran et al., 2015; Drake et al., 2018; Kipp et al., 2018; van der Loeff et al., 2018; Tank et al., 2016; Toohey et al., 2016). The increase in river discharge has the potential to considerably increase trace metal inventories in the future Arctic Ocean, perhaps particularly for those metals that are strongly organically complexed, thus protecting against scavenging in the estuarine mixing zone (Bundy et al., 2015). These increases in metals over time will have implications for metal stoichiometries and phytoplankton growth in a changing Arctic Ocean.”

719-720 an increase in fluvial discharge as well as timing of ice melt could also affect primary productivity on the shelf and thus sedimentary oxygen conditions and Co supply from the sediments (similar to Zn; Jensen et al 2019). And what about increased SGD, could that play a role?

We do not think that SGD could be playing a role here because there are no marine terminating glaciers in this region to our knowledge. Primary production certainly could play a role, and these have been mentioned in this section.

725 I have some issues with this section. First, it is very odd to compare only to the zonal Noble et al. study when in this discussion the comparison to the meridional Dulaquais study would make much more sense as that also has observations much closer to the Arctic (and also states: ‘the LSW was characterized by relatively high DCo concentrations’). This data is available from the IDP. Moreover, LSW is not the only water mass of Arctic origin, also the deeper components of NADW are of Arctic origin (Denmark Strait Overflow Water and Iceland-Scotland Overflow Water). So if LSW is elevated in Co due to its Arctic origin, why is LSW elevated relative to ISOW and DSOW that are also of Arctic origin? This needs to be addressed.

We have added the Dulaquais et al. (2014) reference in this section. We have discussed in this section that the LSW signature is likely a combined signal of Arctic inputs and additional dCo inputs picked up on the shelf in the Labrador Sea, and that is part of the reason why we do not think there is a similarly visible signal in ISOW and DSOW. Additionally, the high dCo is confined to the upper water column in the Arctic and thus is less likely to contribute to these deep water masses. LSW is also fresher and has lower silicate compared to ISOW and DSOW (Jenkins et al. 2015), additionally suggesting an influence from surface waters.

749 not sure what the T-S plot shows/adds or how it supports the hypothesis; basically it shows that dCo is lower in LSW than in the source waters, but you do not need a T-S plot to show this.

We have kept this figure because we think it is the best way to show the two datasets concurrently.

773 where does the Zn data come from? According to the caption it is from this study, but this is the first mention of it. Again the comparison to the GA03 section rather than the more relevant GA02 section is very odd in my opinion as all data is accessible in the IDP and provides data (and insight from the associated publications) much closer to the Arctic. I really urge the authors to make use of the data (and insights) available from the international GEOTRACES efforts.

The Zn data from the Arctic is from Jensen et al. (2019) and S. John (unpublished). The remaining data is from the GEOTRACES IDP 2017. Both Noble et al. (2016) and Dulaquais et al. (2014) observed similar signatures of high dCo in LSW, so we feel like either dataset is appropriate for this comparison. We have now discussed this more thoroughly in this section.

779 quite similar. What is this statement based on given that the medians are more than a factor of 2 apart? I see there is considerable overlap, but not sure if ‘quite similar’ is the observation all readers would make based on the presented graph. Some explanation seems required.

We have changed this to be “similar.”

781 Bit of a jump from Co to total metal concentrations. For metals with different biogeochemistry this might be different and an increase in fluvial supply in the Arctic (of e.g. scavenged Al) might have no consequence for transport to the Atlantic.

We of course acknowledge that there will not be increases in all other trace metals, though it is plausible for those that show similar correlations with shelf and fluvial inputs (Charette et al. 2020).

783-785 do not follow this sentence; the total inventory of Zn is small compared to Zn? And why is the Jensen et al., 2019 only briefly mentioned here? As indicated above, the comparison to the cycling of Zn would have been relevant elsewhere in this ms too.

Here, we were stating that the total inventory of dCo in the ocean is much smaller than dZn, so small changes to dCo sources may have a disproportionate impact compared to increases in dZn fluxes. We have added some discussion of the Zn distributions throughout the manuscript, while being mindful of length.

791-792 This ms has not demonstrated there is any influence of the Co distribution (or the changing Co concentrations) on the Arctic ecosystem, just that Co concentrations could be changing. Moreover, given that Co concentrations are high, I fail to see how a further increase in Co is affecting the ecosystem. And how does the unique Co distribution affect future changes in micro nutrients?

This sentence was meant to highlight the distinct distributions of dCo in this basin compared to other open ocean regions (Figure 3). We also discussed how because the primary sources of dCo in this basin were found to be from a combination of shelf sediments and rivers, and that these sources have been shown to be increasing over time for many other tracers, that it is possible for dCo to continue to change over time as well.

799 as stated before, this cannot be stated like this based on 2 data points in time!

We have clarified throughout the manuscript that we are merely provide intriguing evidence that dCo is increasing over time in the Arctic. We have also added the following sentence in section 4.3, “We recognize these two Arctic dCo datasets are limited in temporal coverage and have methodological differences; however, we felt a responsibility to transparently present these observations of dCo increases in the Arctic Ocean to raise community awareness of this potential environmental change.”

805 similar interpretations were also invoked based on e.g. the micronutrient distributions along the GA02 section (e.g. Cd, Zn, Ni, Fe and Fe binding ligands, Co). I do not mind this is not a completely novel finding, but it is appropriate to acknowledge this idea was postulated before and in fact could strengthen the case for this study on Co.

These other datasets have been mentioned in the preceding section.

Not all figures have units on the axis (color bar fig 8, y axis fig 11) The cited references in the text are not all in reference list

Both have been amended.

References

- Bertrand, E. M., Saito, M. A., Rose, J. M., Riesselman, C. R., Lohan, M. C., Noble, A. E., Lee, P. A. and DiTullio, G. R.: Vitamin B₁₂ and iron colimitation of phytoplankton growth in the Ross Sea, *Limnol. Oceanogr.*, 52(3), 1079–1093, doi:10.4319/lo.2007.52.3.1079, 2007.
- Bertrand, E. M., Allen, A. E., Dupont, C. L., Norden-Krichmar, T. M., Bai, J., Valas, R. E. and Saito, M. A.: Influence of cobalamin scarcity on diatom molecular physiology and identification of a cobalamin acquisition protein, *Proc. Natl. Acad. Sci.*, 109(26), E1762–E1771, doi:10.1073/pnas.1201731109, 2012.
- Bertrand, E. M., McCrow, J. P., Moustafa, A., Zheng, H., McQuaid, J. B., Delmont, T. O., Post, A. F., Sipler, R. E., Spackeen, J. L. and Xu, K.: Phytoplankton–bacterial interactions mediate micronutrient colimitation at the coastal Antarctic sea ice edge, *Proc. Natl. Acad. Sci.*, 112(32), 9938–9943, 2015.
- Browning, T. J., Achterberg, E. P., Rapp, I., Engel, A., Bertrand, E. M., Tagliabue, A. and Moore, C. M.: Nutrient co-limitation at the boundary of an oceanic gyre, *Nature*, 551(7679), 242–246, doi:10.1038/nature24063, 2017.
- Bundy, R. M., Abdulla, H. A. N. N., Hatcher, P. G., Biller, D. V., Buck, K. N. and Barbeau, K. A.: Iron-binding ligands and humic substances in the San Francisco Bay estuary and estuarine-influenced shelf regions of coastal California, *Mar. Chem.*, 173, 183–194, doi:10.1016/j.marchem.2014.11.005, 2015.
- Charette, M. A., Kipp, L. E., Jensen, L. T., Dabrowski, J. S., Whitmore, L. M., Fitzsimmons, J. N., Williford, T., Ulfssbo, A., Jones, E., Bundy, R. M. and others: The Transpolar Drift as a Source of Riverine and Shelf-Derived Trace Elements to the Central Arctic Ocean, *J. Geophys. Res. Ocean.*, 2020.
- Colombo, M., Jackson, S. L., Cullen, J. T. and Orians, K. J.: Dissolved iron and manganese in the Canadian Arctic Ocean: On the biogeochemical processes controlling their distributions, *Geochim. Cosmochim. Acta*, 277(15 May 2020), 150–174, 2020.
- Doxaran, D., Devred, E. and Babin, M.: A 50% increase in the mass of terrestrial particles delivered by the Mackenzie River into the Beaufort Sea (Canadian Arctic Ocean) over the last 10 years, 2015.
- Doxey, A. C., Kurtz, D. A., Lynch, M. D. J., Sauder, L. A. and Neufeld, J. D.: Aquatic metagenomes implicate Thaumarchaeota in global cobalamin production, *ISME J.*, 9(2), 461, 2015.
- Drake, T. W., Tank, S. E., Zhulidov, A. V., Holmes, R. M., Gurtovaya, T. and Spencer, R. G. M.: Increasing alkalinity export from large Russian Arctic rivers, *Environ. Sci. Technol.*, 52(15), 8302–8308, 2018.
- Kipp, L. E., Charette, M. A., Moore, W. S., Henderson, P. B. and Rigor, I. G.: Increased fluxes of shelf-derived materials to the central Arctic Ocean, *Sci. Adv.*, 4(1), eaao1302, 2018.

- van der Loeff, M., Kipp, L., Charette, M. A., Moore, W. S., Black, E., Stimac, I., Charkin, A., Bauch, D., Valk, O., Karcher, M. and others: Radium isotopes across the Arctic Ocean show time scales of water mass ventilation and increasing shelf inputs, *J. Geophys. Res. Ocean.*, 123(7), 4853–4873, 2018.
- Martin, J. H., Gordon, R. M., Fitzwater, S. and Broenkow, W. W.: VERTEX: phytoplankton/iron studies in the Gulf of Alaska, *Deep Sea Res. Part A. Oceanogr. Res. Pap.*, 36(5), 649–680, 1989.
- Moore, C. M., Mills, M. M., Arrigo, K. R., Berman-Frank, I., Bopp, L., Boyd, P. W., Galbraith, E. D., Geider, R. J., Guieu, C., Jaccard, S. L., Jickells, T. D., La Roche, J., Lenton, T. M., Mahowald, N. M., Marañón, E., Marinov, I., Moore, J. K., Nakatsuka, T., Oschlies, A., Saito, M. A., Thingstad, T. F., Tsuda, A., Ulloa, O., Marañón, E., Marinov, I., Moore, J. K., Nakatsuka, T., Oschlies, A., Saito, M. A., Thingstad, T. F., Tsuda, A. and Ulloa, O.: Processes and patterns of oceanic nutrient limitation, *Nat. Geosci.*, 6(9), 701–710, doi:10.1038/ngeo1765, 2013.
- Newton, R., Schlosser, P., Mortlock, R., Swift, J. and MacDonald, R.: Canadian Basin freshwater sources and changes: Results from the 2005 Arctic Ocean Section, *J. Geophys. Res. Ocean.*, 118(4), 2133–2154, 2013.
- Saito, M. A., Rocab, G. and Moffett, J. W.: Production of cobalt binding ligands in a *Synechococcus* feature at the Costa Rica upwelling dome, *Limnol. Oceanogr.*, 50(1), 279–290, 2005.
- Saito, M. A., Goepfert, T. J., Noble, A. E., Bertrand, E. M., Sedwick, P. N. and DiTullio, G. R.: A seasonal study of dissolved cobalt in the Ross Sea, Antarctica: micronutrient behavior, absence of scavenging, and relationships with Zn, Cd, and P, *Biogeosciences*, 7(12), 4059–4082, doi:10.5194/bg-7-4059-2010, 2010.
- Tagliabue, A., Hawco, N. J., Bundy, R. M., Landing, W. M., Milne, A., Morton, P. L. and Saito, M. A.: The role of external inputs and internal cycling in shaping the global ocean cobalt distribution: insights from the first cobalt biogeochemical model, *Global Biogeochem. Cycles*, 32(4), 1–23, doi:10.1002/2017GB005830, 2018.
- Tank, S. E., Striegl, R. G., McClelland, J. W. and Kokelj, S. V: Multi-decadal increases in dissolved organic carbon and alkalinity flux from the Mackenzie drainage basin to the Arctic Ocean, *Environ. Res. Lett.*, 11(5), 54015, 2016.
- Toohey, R. C., Herman-Mercer, N. M., Schuster, P. F., Mutter, E. A. and Koch, J. C.: Multidecadal increases in the Yukon River Basin of chemical fluxes as indicators of changing flowpaths, groundwater, and permafrost, *Geophys. Res. Lett.*, 43(23), 12–120, 2016.

Elevated sources of cobalt in the Arctic Ocean

Randelle M. Bundy^{1,a,*}, Alessandro Tagliabue², Nicholas J. Hawco^{1,4}, Peter L. Morton³, Benjamin S. Twining⁴, Mariko Hatta⁵, Abigail E. Noble^{1,b}, Mattias R. Cape^{1,a}, Seth G. John⁶, Jay T. Cullen⁷ and Mak A. Saito¹

¹Department of Marine Chemistry and Geochemistry, Woods Hole Oceanographic Institution, Woods Hole, MA, USA

²School of Environmental Sciences, University of Liverpool, Liverpool, United Kingdom

³National High Magnetic Field Laboratory, Tallahassee, FL, USA

⁴Bigelow Laboratory for Ocean Sciences, East Boothbay, ME, USA

⁵Department of Oceanography, University of Hawai'i at Manoa, Honolulu, HI

⁶Department of Earth Sciences, University of Southern California, Los Angeles, CA, USA

⁷School of Earth and Ocean Sciences, University of Victoria, Victoria, BC, Canada

^aSchool of Oceanography, University of Washington, Seattle, WA, USA

^bCalifornia Department of Toxic Substances Control, Sacramento, CA, USA

*corresponding author: msaito@whoi.edu

Keywords: cobalt, GEOTRACES, Arctic Ocean, biogeochemical model

Running header: Elevated cobalt in the Arctic

Abstract

Cobalt (Co) is an important bioactive trace metal that is the metal co-factor in cobalamin (vitamin B₁₂) which can limit or co-limit phytoplankton growth in many regions of the ocean. Total dissolved and labile Co measurements in the Canadian sector of the Arctic Ocean during U.S. GEOTRACES Arctic expedition (GN01) and the Canadian International Polar Year-GEOTRACES expedition (GIPY14) revealed a dynamic biogeochemical cycle for Co in this basin. The major sources of Co in the Arctic were from shelf regions and rivers, with only minimal contributions from other freshwater sources (sea ice, snow) and aeolian deposition. The most striking feature was the extremely high concentrations of dissolved Co in the upper 100 m, with concentrations routinely exceeding 800 pmol L⁻¹ over the shelf regions. This plume of high Co persisted throughout the Arctic basin and extended to the North Pole, where sources of Co shifted from primarily shelf-derived to riverine, as freshwater from Arctic rivers was entrained in the Transpolar Drift. Dissolved Co was also strongly organically-complexed in the Arctic, ranging from 70-100% complexed in the surface and deep ocean, respectively. Deep water concentrations of dissolved Co were remarkably consistent throughout the basin (~55 pmol L⁻¹), with concentrations reflecting those of deep Atlantic water and deep ocean scavenging of dissolved Co. A biogeochemical model of Co cycling was used to support the hypothesis that the majority of the high surface Co in the Arctic was emanating from the shelf. The model showed that the high concentrations of Co observed were due to the large shelf area of the Arctic, as well as dampened scavenging of Co by manganese (Mn)-oxidizing bacteria due to the lower temperatures. The majority of this scavenging appears to have occurred in the upper 200 m, with minimal additional scavenging below this depth. These limited temporal results are consistent with other tracers showing increased continental fluxes to the Arctic ocean, and imply both dCo and LCo increasing over time on the Arctic shelf. These elevated surface concentrations of Co likely lead to a net flux of Co out of the Arctic, with implications for downstream biological uptake of Co in the North Atlantic and elevated Co in North Atlantic Deep Water. Understanding the current distributions of Co in the Arctic will be important for constraining changes to Co inputs resulting from regional intensification of freshwater fluxes from ice and permafrost melt in response to ongoing climate change.

Deleted: can limit or co-limit phytoplankton growth in many regions of the ocean.

Deleted: along the transect

Deleted: Preliminary evidence suggests that both dissolved and labile Co are increasing over time on the Arctic shelf, and the elevated surface concentrations of Co likely leads to a net flux of Co out of the Arctic, with implications for downstream biological uptake of Co in the North Atlantic and elevated Co in North Atlantic Deep Water. Understanding the current distributions of Co in the Arctic will be important for constraining changes to Co inputs resulting from regional intensification of freshwater fluxes from ice and permafrost melt in response to ongoing climate change.

1. Introduction

Cobalt (Co) is an essential micronutrient in the ocean. It is utilized by eukaryotic phytoplankton as a substitute for zinc (Zn) in the metalloenzyme carbonic anhydrase (Lane and Morel, 2000; Sunda and Huntsman, 1995; Yee and Morel, 1996), and cyanobacteria have an absolute requirement for Co (Hawco and Saito, 2018; Saito et al., 2002; Sunda and Huntsman, 1995). Co is also the metal center in the micronutrient cobalamin, or vitamin B₁₂. In most ocean basins, dissolved Co (dCo; < 0.2 µM) is extremely scarce in surface waters (< 10 pmol L⁻¹), and is strongly complexed by a pool of thus far uncharacterized organic Co-binding ligands (Saito et al., 2005; Saito and Moffett, 2001). Due to its low concentrations, strong organic complexation, and its presence in cobalamin, dCo or cobalamin have been found to be the limiting or co-limiting nutrient for phytoplankton growth in several regions (Bertrand et al., 2007, 2015; Browning et al., 2017; Hawco et al., 2020; Martin et al., 1989; Moore et al., 2013; Panzeca et al., 2008; Saito et al., 2005). Growth limitation can be due to either a lack of dCo, or cobalamin (Bertrand et al., 2012; Bertrand et al., 2007; Browning et al., 2017), as cobalamin is only synthesized by cyanobacteria and some archaea (Doxey et al., 2015). However, many phytoplankton utilize cobalamin for the synthesis of methionine (Yee and Morel, 1996; Zhang et al., 2009), and therefore must obtain it from the natural environment (Heal et al., 2017).

Co is taken up as a micronutrient by phytoplankton in surface waters and is regenerated from sinking organic matter at depth, but it is also prone to intense scavenging throughout the mesopelagic ocean (Hawco et al., 2018; Saito et al., 2017). The strongest removal mechanism for dissolved Co (dCo) is through co-precipitation of dCo with manganese (Mn) by Mn-oxidizing bacteria, due to their similar redox properties and ionic radii (Cowen and Bruland, 1985; Moffett and Ho, 1996; Sunda and Huntsman, 1988). Several sources of Co to the ocean have been identified, including riverine (Tovar-Sánchez et al., 2004; Zhang et al., 1990), coastal sediments (Hawco et al., 2016; Noble et al., 2012; Noble et al., 2017), and to a lesser extent hydrothermal and aeolian inputs (Shelley et al., 2012; Thuróczy et al., 2010). The largest reservoirs of dCo thus far have been seen in oxygen deficient zones, likely due to a combination of low oxygen concentrations at the sediment-water interface and advection from reducing sediments, as well as enhanced regeneration in low oxygen waters (Dulaquais et al., 2014b; Hawco et al., 2016; Noble et al., 2012, 2016). These oxygen minimum zone sources of dCo exert an important control on the inventory of dCo, which is likely sensitive to small perturbations in bottom water oxygen concentrations (Hawco et al., 2018; Tagliabue et al., 2018).

It is important to understand the sources and sinks and internal cycling of dCo due to its important role as a micronutrient. However, Co has one of the most complex biogeochemical cycles of all of the trace metals. Thousands of measurements of both total dCo and weakly complexed and/or inorganic or “labile” Co (LCo) and particulate Co (pCo) now exist in the ocean, greatly improving our understanding of Co cycling and have facilitated the representation of the biogeochemical model of Co to be included in global ocean models (Tagliabue et al., 2018). Several observational zonal transects have been generated by large-scale programs including the international GEOTRACES program, among others. Large datasets now exist in the North Atlantic (Baars and Croot, 2015; Dulaquais et al., 2014a; Dulaquais et al., 2014b; Noble et al., 2017), South Atlantic (Noble et al., 2012), South Pacific (Hawco et al., 2016),

Deleted: and

Deleted: has

Southern Ocean (Bown et al., 2011; Saito et al., 2010), and Mediterranean Sea (Dulaquais et al., 2017).

Although the global coverage of Co measurements has greatly improved over the last decade, no published measurements to our knowledge have been made in the Arctic Ocean. The Arctic Ocean is arguably the most dynamic of the ocean basins, and is changing rapidly due to warmer temperatures affecting the maximal sea ice extent (Screen and Simmonds, 2010; Stroeve et al., 2012), the melting of permafrost (Jorgenson et al., 2006), and additional inputs of meltwater and river water (Johannessen et al., 2004; Serreze and Barry, 2011). The Arctic Ocean is also likely distinct in terms of Co cycling compared to other ocean basins due to its large shelf area, restricted circulation, and potentially distinct Co sources including sea ice, snow, and highly seasonal riverine inputs. The Arctic Ocean is known to have high concentrations of dissolved organic matter (DOM), which could influence the organic complexation of Co in this ocean basin. **This study examined dCo, LCo, and pCo in two different transects in the Canadian sector of the Arctic Ocean.** We then used a Co biogeochemical model (Tagliabue et al., 2018) in order to **evaluate hypotheses about the role of external sources and internal cycling to the observed Co distributions, the potential of the Arctic to be a net source of Co to the North Atlantic, and to identify Co sources and sinks that may be sensitive to future changes in this rapidly changing ocean basin.**

2. Methods

2.1 Sample collection and handling

2.1.1. Water column samples

Samples were collected on two expeditions in the Canadian section of the Arctic Ocean (Fig. 1). The first set of samples ($n = 107$) were collected on board the CCGS *Amundsen* from August 27, 2009 to September 12, 2009 in the Beaufort Sea as part of the Canadian IPY-GEOTRACES program (ArcticNet 0903; GIPY14). The second set of samples ($n = 361$) were collected on board the USCGC *Healy* (HLY1502) on the U.S. GEOTRACES Arctic expedition (GN01) from August 9, 2015–October 12, 2015. The Canadian GEOTRACES expedition sampled along the shelf and slope in the Beaufort Sea. The U.S. GEOTRACES expedition sailed in and out of Dutch Harbor, Alaska, and traversed across the Bering Shelf and Makarov Basin before reaching the North Pole on September 5, 2015 and returning south across the Canada Basin. Samples from the Canadian GEOTRACES expedition were collected using a trace metal rosette system fitted with 12 x 12 L GO-FLO bottles (General Oceanics), and only the dCo and LCo samples collected in the water column from this study are discussed here. All other metadata from this expedition can be found at <http://www.bodc.ac.uk/geotraces/data/>. Samples from the U.S. GEOTRACES expedition were collected using the U.S. GEOTRACES trace metal clean rosette outfitted with twenty-four 12 L GO-FLO bottles and a Vectran conducting hydrowire (Cutter and Bruland, 2012). Two GO-FLO bottles were triggered at each depth during the trace metal hydrocasts. One bottle was used for particulate trace metal sampling, and the other was used for all dissolved metal and macronutrient analyses. Upon recovery of the sampling system, the GO-FLO bottles were immediately brought inside a twenty-foot ISO container van. Sampling for bulk particulate trace metal samples has been described in detail elsewhere (Twining et al., 2015). The filters were stored in trace metal clean centrifuge tubes and frozen at -20°C until

Deleted: While these studies document certain features in dCo distributions that are common in all basins, there exist unique, regionally specific features. For example, although several of the datasets included regions influenced by hydrothermal inputs, no significant Co feature associated with the neutrally buoyant plume was observed (Hawco et al., 2016) and only a small point source of dCo was observed in another case (Noble et al., 2016). Additionally, strong nepheloid layers were shown to be a bottom water sink for dCo (Noble et al., 2016).

Deleted: This study examined two distinct transects of dCo, LCo and one transect of pCo in the Canadian sector of the Arctic Ocean.

Deleted: interpret the role of external sources and internal cycling to the observed Co distributions, the potential of the Arctic to be a net source of Co to the North Atlantic, and to identify Co sources and sinks that may be sensitive to future changes in this rapidly changing ocean basin.

Deleted: Briefly, samples were filtered with 25 mm Supor 0.45 μm polyethersulfone filters mounted in Swinnex polypropylene filter holders (Twining et al., 2015). After filtering, the volume that passed through the filter was measured and a vacuum was applied to remove any remaining seawater on the filters.

analysis (Twining et al., 2015). Dissolved trace metal and nutrient samples were filtered with a 0.2 μm capsule filter (Acropak-200, VWR International) under pressurized filtered air (Cutter and Bruland, 2012). Samples for dCo and LCo from the Canadian GEOTRACES expedition were collected similarly, but were unfiltered. Samples for dCo were placed in two separate 60 mL Citranox-soaked (1%) and acid-cleaned low-density polyethylene (LDPE) bottles and were filled until there was no head space (Noble et al., 2012; Noble et al., 2017). One sample was used for LCo analyses and the other was used for total dCo analyses. Nutrient samples were analyzed immediately on-board by the Ocean Data Facility at Scripps Institution of Oceanography.

Deleted: Nutrient samples were analyzed immediately on-board by the Ocean Data Facility at Scripps Institution of Oceanography. Samples for dCo were placed in two separate 60 mL Citranox-soaked (1%) and acid-cleaned low-density polyethylene (LDPE) bottles and were filled until there was no head space (Noble et al., 2012; Noble et al., 2017). One sample was used for LCo analyses and the other was used for total dCo analyses.

2.1.2 Ice hole samples

Ice hole samples were only analyzed from the U.S. GEOTRACES cruise (GN01). Seawater from ice holes for Co analyses was collected using Teflon coated Tygon tubing and a rotary pump with plastic wetted parts (IWAKI magnetic drive pump, model WMD-30LFY-115) from a hole at the station's sea ice floe. The hole was made with an ice corer (Kovacs 9 cm diameter Mak II corer), and allowed to sit undisturbed for ~ 1 hour under a canvas tent prior to sampling. Samples were collected from 1, 5 or 20 m at several sites. Seawater was filtered in-line with a 0.2 μm filter (Acropak-200 capsule filter) and dispensed into a carboy, where it was homogenized and brought back to the clean lab on board the ship. Sub-samples were taken for dCo from this carboy, and stored as described below for other water column dissolved samples. Additional details on ice hole samples can be found elsewhere (Marsay et al., 2018).

2.2 Sample storage

Total dCo and LCo samples were stored in two distinct ways. Oxygen concentrations have been found to have a significant effect on storage of dCo samples (Noble et al., 2017). Although the mechanism has not been fully explained, loss of some dCo species has been observed in the presence of oxygen on both acidified and non-acidified samples across regions with active biological gradients (Hawco et al., 2016; Noble et al., 2012; Noble et al., 2017, 2008). Since dCo and LCo analyses were not able to be performed at sea on either expedition, groups of six dCo samples from the U.S. expedition from a single cast were double-bagged and stored in a gas-impermeable plastic bag (Ampac) along with 3-4 gas-absorbing satchels (Mitsubishi Gas Chemical- model RP-3K). This outer bag was heat-sealed and samples were kept refrigerated (4°C) and un-acidified until analysis (Hawco et al., 2016, 2018; Noble et al., 2016). LCo samples were double-bagged and stored at 4°C and un-acidified until analysis. Samples were hand-carried at the termination of the GN01 expedition to Woods Hole Oceanographic Institution, and all samples were analyzed within three months. Samples from the Canadian GEOTRACES expedition (GIPY14) were collected as unfiltered samples prior to filtration and analysis, and were not stored in gas-impermeable bags prior to analysis, as the effects of oxygen on dCo loss were not known at the time of the expedition. It is possible there could have been some loss of dCo during the time between sample collection and analyses (approximately one year), and thus these concentrations could be underestimated. Additional discussion on how storage may have impacted these results is discussed in section 3.2.2 and 4.3.

Deleted: until

Deleted: ,

2.3 Reagent preparation

218 All reagents were prepared in acid-clean plastic bottles and in large batches in order to have
 219 consistent reagent batches for all sample analyses. For dCo and LCo analyses, a 0.5 mol L⁻¹
 220 EPPS (N-(2-hydroxyethyl)piperazine-N-(3-propanesulfonic acid)) buffer and a 1.5 M NaNO₂
 221 solution were prepared in Milli-Q (18 MΩ) and chelexed (Chelex-100, Biorad) to remove trace
 222 metal contaminants. Dimethylglyoxime (DMG) was prepared by first making a 10⁻³ mol L⁻¹
 223 EDTA solution in Milli-Q and adding 1.2 g of DMG. This solution was warmed by carefully
 224 microwaving at 50% power to prevent boiling, until the DMG was fully dissolved. The solution
 225 was placed on ice and left at 4°C to recrystallize overnight. The supernatant was decanted, and
 226 the remaining crystals were poured into an acid-cleaned plastic weigh boat and the remaining
 227 liquid was left to evaporate overnight in a Class-100 clean hood. Once dry, the remaining DMG
 228 was added to an Optima methanol solution for a final concentration of 0.1 mol L⁻¹ DMG. A 1.5
 229 mol L⁻¹ solution of sodium nitrite was prepared by placing sodium nitrite in Milli-Q and
 230 chelexing the solution before use to remove trace metal contaminants. A Co standard solution
 231 was prepared weekly by adding 29.5 µl of a 1 mg L⁻¹ Co AA standard (SPEX CertiPrep) to 100
 232 mL of Milli-Q in a volumetric flask. For each new Co standard that was prepared during sample
 233 runs, an approximately 1 mL aliquot was saved for later analyses to ensure no variation was seen
 234 between batches. More information on reagent preparations can be found at
 235 <https://www.protocols.io/researchers/randie-bundy/publications>.

Deleted: ,

Deleted: prior to analyses

Deleted: of each reagent were made

237 2.4 Dissolved and labile cobalt determinations

239 The dCo and LCo measurements were determined using a modified cathodic stripping
 240 voltammetry method (Saito and Moffett, 2001) for the GIPY14 samples, and a fully automated
 241 method based on Hawco et al. (2016) for the GN01 samples (Hawco et al., 2016). Measurements
 242 for both sample sets were performed using a Metrohm 663 VA stand connected to an Eco-
 243 Chemie µAutolabIII system. Peak determinations for samples collected on GIPY14 were
 244 completed as described in Noble et al. (2012). Sample automation and data acquisition for
 245 samples from GN01 was completed using NOVA 1.8 software (Metrohm Autolab), and peak
 246 determination was completed using a custom MATLAB code (see section 2.6).

248 The dCo samples were UV-irradiated for one hour in a temperature-controlled UV system prior
 249 to analysis to remove any strong organic ligands that may prevent DMG from effectively binding
 250 the entire dCo pool. For the GIPY14 samples, a modified temperature controlled UV system
 251 (Metrohm 705 Digestor) was used (Hawco et al., 2016), while for GN01 samples an integrated
 252 temperature-controlled (18°C) digestor was used (Metrohm 909 Digestor). In both cases samples
 253 were placed in acid-cleaned and Milli-Q conditioned 15 mL quartz tubes. After irradiation, 11
 254 mL of each sample was placed into acid-cleaned and sample-rinsed 15 mL polypropylene tubes.
 255 For GIPY14 samples a final concentration of 353 µmol L⁻¹ DMG and 3 mmol L⁻¹ EPPS was
 256 added to each sample before analysis (Noble et al., 2016), and for GN01 samples a final
 257 concentration of 400 µmol L⁻¹ DMG and 7.6 mmol L⁻¹ EPPS was added to each sample before
 258 analysis. Samples were then inverted several times before either being analyzed individually or
 259 being placed on the autosampler (Metrohm 858 Sample Processor). For autosampler analyses,
 260 the system was flushed with Milli-Q and 2 mL of sample were used to condition the tubing and
 261 the Teflon analysis cup. Then 8.5 mL of sample was dosed into the cup automatically by a
 262 Dosino 800 burette (Metrohm), along with 1.5 mL addition of 1.5 M NaNO₂ for a final analysis
 263 volume of 10 mL. Samples were purged for 180 s with N₂ (high purity, > 99.99%) and

267 conditioned at -0.6 V for 90 s. The inorganic Co in the sample that was complexed by DMG
268 ($\log K^{cond} = 11.5 \pm 0.3$) forms a bis-complex with Co^{2+} that absorbs to the hanging mercury drop
269 electrode (Saito and Moffett, 2001). The Co^{2+} and the DMG are both reduced at the electrode
270 surface using a fast-linear sweep (from -0.6 V to -1.4 V at 10 V s^{-1}) and the height of the
271 Co(DMG)_2 reduction peak that appears at -1.15 V is proportional to the dCo concentration in the
272 sample. The dCo was quantified by triplicate scans of the sample, followed by four standard
273 additions of either 25 or 50 pmol L^{-1} per addition that were dosed directly into the Teflon
274 analysis cup. The slope of the linear regression of these additions and triplicate “zero” scans
275 were used to calculate the individual sample-specific sensitivity ($\text{nA pmol}^{-1} \text{ L}^{-1}$). The average of
276 the three “zero addition” scans was then divided by the sensitivity and then corrected for the
277 volume of the reagent, and the blank (see section 2.5). In between sample batches, or before
278 analyzing LCo samples, the entire auto-sampling system was rinsed with 10% HCl and then
279 Milli-Q.

280
281 LCo measurements were made similarly to the dCo measurements, with the following
282 amendments. LCo samples were not UV-irradiated, and 400 $\mu\text{mol L}^{-1}$ DMG was added to 11 mL
283 of sample and was equilibrated for at least 8 hours (overnight) in conditioned 15 mL
284 polypropylene tubes. Immediately prior to placement of the sample on the autosampler, EPPS
285 was added and the samples were analyzed as described above for dCo analyses. LCo
286 measurements are thus operationally defined as the fraction of dCo that is labile to 400 $\mu\text{mol L}^{-1}$
287 DMG over the equilibration period (Hawco et al., 2016; Noble et al., 2012).

288 289 2.5 Blanks and standards

290
291 The blank for GN01 samples was prepared by UV-irradiating low dCo seawater for one hour.
292 After UV-irradiation, the seawater was passed slowly through a Chelex-100 column to remove
293 any metals. The clean seawater was then UV-irradiated a second time before being analyzed. The
294 blank used for GIPY14 samples was analyzed at the beginning and the end of the sample
295 analyses to ensure the blank was consistent between runs. GEOTRACES consensus reference
296 materials were also analyzed along with GIPY14 samples, the results of which are reported
297 elsewhere (Noble et al., 2016).

298
299 For the GN01 samples, enough seawater was prepared in order to use the same blank seawater
300 for all of the subsequent sample analyses and the blank was analyzed regularly with each batch
301 of samples (every 10-20 samples). A combination of consensus reference materials and an in-
302 house seawater consistency standard were used throughout the sample analyses (Table 1). SAFe
303 and GEOTRACES standards were analyzed to ensure the accuracy of the sample measurements,
304 and were slowly neutralized drop wise with 1 N ammonium hydroxide (Optima, Fisher
305 Scientific) until reaching a pH of approximately 8. Aliquots of the SAFe and GEOTRACES
306 samples were then placed in conditioned quartz tubes and UV-irradiated for one hour, before
307 being analyzed as described above for dCo measurements. The consistency standard was
308 prepared by UV-irradiating 2 L of Southern Ocean trace metal clean seawater as described above
309 and was analyzed with each batch of samples to ensure consistency between sample runs.

310 311 2.6 Dissolved and labile cobalt data processing

312

Deleted: ¶
¶

315 Peak heights for the dCo and LCo samples for the GIPY14 dataset were determined in NOVA
316 1.8 software (Noble et al., 2016). All dCo and LCo peaks from the GN01 dataset were calculated
317 using custom MATLAB code available on GitHub (<https://github.com/rmbundy/voltammetry>).
318 Text files of the data output from NOVA 1.8 software were saved automatically from each scan,
319 and processed in MATLAB to determine the dCo and LCo peak heights. The signal was
320 smoothed using the Savitzky-Golay smoothing function (span 5, degree 3), and the first
321 derivative of the voltammetric signal between -1.4 and -1.1 V was calculated in order to find the
322 start and end of the Co(DMG)₂ peak. The baseline was drawn and linearly interpolated between
323 the start and the end of the peak. The final peak height was determined by finding the maximum
324 of the signal and subtracting it from the baseline. Peak heights from the “zero addition” scans
325 were plotted along with the standard additions, and a linear regression was computed from all
326 seven scans. Data was flagged if the r^2 of the slope was < 0.97 , and samples were re-analyzed.

327 2.7 Dissolved and particulate manganese measurements

328
329 The 0.2 μm -filtered seawater samples for dissolved manganese (dMn) were acidified to pH 2
330 using sub-boiling distilled HCl. The filtered subsamples were drawn into acid pre-washed 125
331 mL polymethylpentene bottles after three sample rinses, and the sample bottles were stored in
332 polyethylene bags in the dark at room temperature before analyses, which was usually within 24
333 h of collection. Prior to analysis, samples for manganese (dMn) were acidified by adding 125 μL
334 sub-boiling distilled 6 N HCl. Since the samples were used to determine dissolved iron (dFe) as
335 well, the obtained samples were then microwaved in groups of 4 for 3 min in a 900 W
336 microwave oven to achieve a temperature of $60 \pm 10^\circ\text{C}$ in an effort to release dFe from
337 complexation in the samples. Samples were allowed to cool for at least 1 h prior to flow injection
338 analysis. The dMn measurements were determined in the filtered, acidified, microwave-treated
339 subsamples using shipboard flow inject ion analysis (FIA) method (Resing and Mottl, 1992).
340 Samples were analyzed in groups of 8, and the samples collected at each station were generally
341 analyzed together during the same day. A 3-minute pre-concentration of sample (~ 9 ml) onto an
342 8-hydroxyquinoline (8-HQ) resin column yielded a detection limit of 0.55 nmol L^{-1} and a
343 precision of 1.16% at 2.7 nmol L^{-1} .

344
345 Particulate trace element concentrations were determined through a total digestion procedure as
346 described in Ohnemus et al. (2014) and Twining et al. (2015). Briefly, approximately 7 L of
347 contamination-free seawater were filtered directly from Teflon-coated GO-Flo sampling bottles
348 over acid-washed 47-mm (shelf stations) or 25-mm (open basin stations) PES Supor filters.
349 Filters were divided in half, and one half was digested for 3 hours at $100\text{--}120^\circ\text{C}$ in sealed Teflon
350 vials containing 4 M HCl, 4 M HNO_3 , and 4 M HF (Fisher Optima), which digests the marine
351 suspended particulate matter (SPM) but leaves the PES filter mostly intact. The PES filters were
352 rinsed with ultrahigh purity water ($18.2 \text{ M}\Omega \text{ cm}^{-1}$) and removed from the digestion vials, and 60
353 μL of sulfuric acid (Optima) and 20 μL of hydrogen peroxide (Fisher Optima) were added to the
354 vials to digest any filter fragments. The digest solution was taken to dryness at $\sim 210^\circ\text{C}$ (8-24
355 hours). The digest residue was re-dissolved in 4 mL of 0.32 M HNO_3 before measuring the total
356 particulate Co, Mn and phosphorous (pCo, pMn, pP) concentrations by inductively coupled
357 plasma mass spectrometry (ICP-MS; Thermo Element 2, National High Magnetic Field
358 Laboratory, Tallahassee, Florida). Major and trace element concentrations were calibrated using

Deleted: d

an external multi-element standard curve and corrected for instrument drift using a 10 ppb indium internal standard (Twining et al., 2019).

2.8 Biogeochemical modeling of Co in the Arctic

Modeling runs in the Arctic Ocean were completed using a previously published biogeochemical model for Co (Tagliabue et al., 2018). Briefly, the Co model is part of the PISCES-v2 model and has an additional six tracers for Co, including dCo, scavenged Co (associated with Mn oxides), Co within diatoms, Co in nanoplankton, small particulate organic Co, and large particulate organic Co (Tagliabue et al., 2018). [Phytoplankton uptake of Co in the model allows for variable Co/C ratios and are based on a maximum cellular quota](#). The PISCES model is an excellent platform for these studies as it has a detailed representation of ocean biogeochemical cycling and has been used for a range of different studies. Measured pCo is equal to the sum of all of the particulate Co tracers in the model (including living and non-living pools). Excretion of Co is also simulated in a similar manner as Fe in PISCES-v2, with a fixed Co/C ratio in both micro- and meso-zooplankton that sets the excretion of dCo as a function of the Co content of their food (Tagliabue et al., 2018). The background biogeochemical model presented in Tagliabue et al. (2018) was modified slightly for this work, most notably an improved particle flux scheme (Aumont et al., 2017), with the Co specific parameterizations left unchanged. We used the model to assess the role of different processes by conducting sensitivity tests whereby the sedimentary Co source was eliminated, the riverine Co source was eliminated, the slowdown of Co scavenging at lower oxygen was removed (meaning oxygen did not affect Co scavenging) and the change in Co scavenging due to variations in bacterial biomass was instead set to a constant value. By comparing the results of these four sensitivity experiments to the control model, we were able to quantify the relative contributions of different external sources and internal cycling processes.

3. Results

3.1 Oceanographic context

The Arctic Ocean is a unique ocean basin. The surface circulation in the Arctic is characterized by a clockwise current that entrains shelf water from the Chukchi and Eurasian shelves, before being swept across the North Pole by the Transpolar Drift (TPD; Fig. 1). This current is distinguished by its low salinity and elevated concentrations of dissolved organic carbon (DOC) (Klunder et al., 2012; Wheeler et al., 1997). The Arctic Ocean is a highly stratified system, with little mixing between the major water masses (Steele et al., 2004). The major water masses that enter the Arctic through the Bering Strait are the upper modified Pacific water (mPW) and the Pacific halocline water (PHW). The mPW includes inputs from the Bering shelf, as well as freshwater inputs from rivers, sea ice melt, and glacially modified waters. PHW includes some influences from Bering Sea water (BSW; including both summer and winter water (Steele et al., 2004)). Atlantic water (AW) comprises the bulk of the intermediate and deep waters of the Arctic basin. These major water masses (mPW, PHW, AW) can be distinguished from the high-resolution nutrient, oxygen and salinity data from the conventional CTD rosette stations in the sampling region (Fig. 2). The mPW is characteristic of low salinity ($31 < S < 32$) and nutrients (Fig. 2), and contains contributions from Alaskan Coastal Water (Steele et al., 2004), as well as

Deleted: -

Deleted: iron (

Deleted:)

other modified water masses from the shelf. The PHW can be clearly identified from the elevated macronutrient concentrations (Fig. 2D), and temperature maximum within the salinity range of 31-33 (Steele et al., 2004; Steele and Boyd, 1998) (Fig. 2A, C). The AW comprises a relatively uniform deep layer throughout the entire Arctic basin. AW enters the Arctic through the Fram Strait and Barents Sea and cycles in a cyclonic direction around the Eurasian Basin and Canadian Basin (Aagaard and Carmack, 1989; Carmack et al., 1995) and is characterized by higher salinities (> 33), its temperature ($\sim -1.0^{\circ}\text{C}$) and lower nutrient concentrations (silicate $< 5 \mu\text{mol L}^{-1}$).

Deleted: that extend from both shelf regions, but do not quite reach the stations in the vicinity of the North Pole (stations 27-37). PHW can be identified both by its elevated nutrient concentrations, as well as a

3.2 Dissolved cobalt distributions

3.2.1 Elevated dissolved cobalt in surface waters

Blank and consensus values for the GIPY14 dataset are reported elsewhere (Noble et al., 2016) and the dCo blanks and standards for the GN01 analyses are reported in Table 1. The dCo profiles in the Arctic resembled a “scavenged-like” profile throughout the majority of the transect and were distinct from recent U.S. GEOTRACES efforts in the North Atlantic (Noble et al., 2016) and Eastern Tropical South Pacific (Hawco et al., 2016; Fig. 3). When median dCo concentrations from this study are binned by depth, the upper 50 m in the Arctic contains a median dCo concentration approximately 10 times higher than that of surface waters in the North Atlantic or South Pacific (Dulaquais et al., 2014; Hawco et al., 2016; Noble et al., 2017, 2012). Profiles in the Arctic also show no perceptible mid-depth maximum analogous to either the Atlantic or Pacific (Fig. 3), and instead dCo concentrations rapidly decline until reaching values of approximately 50-60 pmol L^{-1} . These concentrations in deep waters are slightly lower than the deep Atlantic and closer to background Pacific levels ($\sim 30\text{-}40 \text{ pmol L}^{-1}$).

The dCo distributions were highly elevated in surface waters ($< 100 \text{ m}$) in the shelf regions (Fig. 4A-C, P-R) and these high concentrations persisted out into the basin in the vicinity of the North Pole (Fig. 4F-H). In the Bering Sea, dCo in surface waters ranged from 131-156 pmol L^{-1} in the upper 40 m, with an apparent surface or sub-surface minimum associated with biological drawdown (Fig. 4A). Concentrations notably increased in stations near the Bering Strait (stations 2-6; Fig. 4B), where dCo reached up to 457 pmol L^{-1} in surface waters (Fig. 4B; Fig. 5), and was even higher in bottom waters, sometimes exceeding 1.5 nmol L^{-1} (Fig. 4B; Fig. 5). Surface enrichment of dCo was even more pronounced on the Chukchi shelf, where concentrations consistently exceeded 800 pmol L^{-1} (Fig. 4Q; Fig. 5). The dCo and LCo concentrations from the Canadian GEOTRACES expedition in 2009 also had near surface maxima in dCo and LCo, with up to 300 pmol L^{-1} dCo (Fig. 4R). These concentrations were lower than nearby samples collected in 2015 (Fig. 4P, Q), which contained up to three times more dCo in the upper 100 m.

Deleted: significantly

The elevated dCo concentrations on both shelves traversed by the U.S. expedition persisted throughout the marginal ice zone (MIZ; stations 12-17, 51-54) and into the Canada basin (stations 12-26), following similar patterns in dFe and dMn (L. Jensen and M. Hatta pers. comm.). Water mass fractions and sea ice melt in the MIZ in this study were determined based on $\delta^{18}\text{O}$ data (Newton et al., 2013). Some high concentrations of dCo were observed in the region of the MIZ and in samples with pronounced influence from meltwater ($> 1.5\%$ sea ice melt; Table 2) in the upper 30 m, with median dCo concentrations equal to 358 pmol L^{-1} in the

Deleted: 7.5

MIZ, though with large variability (range 26-546 pmol L⁻¹) likely due to surface drawdown and additional dCo sources. Surface concentrations in this region ranged from approximately 100-500 pmol L⁻¹ (Fig. 4D-F, M-N). The dCo in surface waters decreased slightly in the Makarov Basin and reached some of the lowest observed concentrations at the North Pole (210 pmol L⁻¹; Fig. 4H; Fig. 5), though concentrations were still slightly higher than at Station 1, the only Pacific station (Fig. 4A). Although some elements such as dFe showed noticeable elevated concentrations in the vicinity of North Pole in surface waters compared to surrounding waters (L. Jensen, pers. comm.), dCo remained lower than on the shelf and in the MIZ (Fig. 5). Surface dCo at the North Pole was approximately 250 pmol L⁻¹, nearly half the concentrations observed in the Canada Basin (Fig. 4H).

3.2.2 Dissolved cobalt in Pacific halocline and deep waters

While silicate (SiO₃) and phosphate (PO₄³⁻) concentrations were indicative of the advection of PHW (Fig. 2E, F), dCo did not show a prominent enhancement within this feature (Fig. 5A), likely due to the slightly lower relative concentrations of dCo in Pacific waters compared to shelf waters (station 1; Fig. 4A). Median concentrations of dCo in waters dominated by Pacific water (> 95%) were 270 pmol L⁻¹ (range 64-687 pmol L⁻¹) while on the shelf they were 526 pmol L⁻¹ (Table 2). Any elevated dCo concentrations observed within the PHW density layer (σ_θ = 26.2-27.2; Steele et al., 2004) was likely added along the flow path of Pacific water across the Bering Shelf (Fig. 4B). Thus, stronger relationships were observed with other elements which are also elevated on the shelf (e.g. dFe and dMn; M. Hatta pers. comm.) than with SiO₃ or other macronutrients (e.g. PO₄³⁻).

The dCo was remarkably constant within the deep Arctic, reflective of both AW and deep Arctic bottom water (Fig. 5A; Swift et al., 1983). Concentrations in AW (> 95% AW, and all depths > 500 m) had a median value of 62 pmol L⁻¹ (Table 2), in between the average deep water dCo concentrations found in the Pacific and Atlantic (Fig. 3). The near-bottom sample from some profiles also showed slightly lower dCo (< 5 pmol L⁻¹) than the sample immediately above it (Fig. 4C, D, F), perhaps indicating some influence of the weak nepheloid layers on bottom-water scavenging of dCo in the Arctic (Noble et al., 2016).

3.3 Labile cobalt distributions

3.3.1 Labile cobalt in surface waters

LCo is the fraction of total dCo that is either not organically complexed or weakly bound by organic ligands, and represents the “labile” fraction of the total dCo pool either in terms of biological uptake or scavenging (Saito et al., 2004; Saito and Moffett, 2001). LCo distributions looked remarkably similar to dCo in the upper water column (Fig. 4, 5). Concentrations were lower than dCo, ranging from 0 (not detectable) to 600 pmol L⁻¹ on the Canadian side of the Chukchi Shelf (station 61, 66). LCo comprised 20-35% of the total dCo pool in the upper water column (Fig. 6), with the highest percentage of LCo found over the Chukchi shelf and approximately 20% LCo in Pacific waters (station 1; Fig. 6). LCo decreased more rapidly with respect to distance from the shelf than dCo in the Canada Basin and towards the North Pole, with the North Pole region containing significantly lower median concentrations of LCo (10 pmol L⁻¹,

Deleted: 5.9

Deleted: .2

Deleted: 269.6

Deleted: .1

Deleted: .3

Deleted: .0

Deleted: 1.6

Deleted: .3

516 $p < 0.05$) than surrounding waters (148 and 117 pmol L⁻¹ on the shelf and MIZ, respectively;
 517 Table 2). The majority of the LCo appeared to either be removed via scavenging or biological
 518 uptake in the upper water column in the Canada Basin and along the Lomonosov Ridge. Some of
 519 the highest median LCo concentrations were observed in the upper 30 m in the MIZ and in
 520 waters containing significant sea ice melt (> 1.5%, Table 2), with median concentrations rivaling
 521 those on the shelf (Table 2). The LCo in these samples had a large range in many cases (49-233
 522 pmol L⁻¹ in samples with > 1.5% sea ice melt), suggesting that sea ice may be a source of LCo,
 523 and that it is taken up quickly in surface waters after input from meltwater.

Deleted: .0

Deleted: .0

Deleted: 8.8

Deleted: .0

525 3.3.2 Labile cobalt in Pacific halocline waters and deep waters

527 LCo was extremely low, and often undetectable, in the deep waters of the Arctic (Fig. 4). Any
 528 detectable LCo at these depths represented less than 10% of total dCo (Fig. 6), with the majority
 529 of the dCo in the deep Arctic was strongly organically complexed. Similar to dCo, there was no
 530 observable enhancement of LCo in PHW, with LCo closely following that of dCo and other
 531 shelf-enhanced trace metals such as dFe and dMn (L. Jensen, pers. comm.; Jensen et al., 2019;
 532 Tonnard et al., 2020). LCo decreased below the upper 250 m, and the median concentration of
 533 LCo in the Atlantic layer was 2 pmol L⁻¹ (Table 2) virtually equal to the detection limit of the
 534 method, suggesting scavenging or uptake of LCo in the upper water column and little to no
 535 detectable LCo in deep waters of the Arctic.

Deleted: (

Deleted:)

Deleted: .2

Deleted: (2.1 pmol L⁻¹)

537 3.4 Dissolved and particulate manganese and particulate cobalt distributions

539 DCo and dMn had very similar distributions across the transect. The pCo and pMn
 540 concentrations were slightly decoupled from the dissolved concentrations, with a subsurface
 541 peak in both (Fig. 7), as opposed to the surface peak observed in dCo and dMn. The maximum in
 542 pCo and pMn occurred at depths of approximately 200-300 m, corresponding to a region of
 543 significantly elevated concentrations of particulate Mn-oxides (P. Lam pers. comm.). Overall,
 544 pCo and pMn concentrations were the highest on the shelf, with visible increases at the base of
 545 the profiles near the sediment water interface (Fig. 7B, C). Concentrations of pCo and pMn
 546 declined by almost an order of magnitude from the shelves into the Arctic basin, with
 547 concentrations ranging from 20-40 pmol L⁻¹ and 1-10 nmol L⁻¹ for pCo and pMn, respectively.
 548 Deep water (> 1000 m) particulate concentrations for both metals were remarkably consistent,
 549 with concentrations varying slightly over the entire Arctic basin (Fig. 7D, H). These deep water
 550 pMn and pCo concentrations are notably higher than in other regions, such as deep Pacific
 551 waters (Lee et al., 2018).

Deleted: (Hatta et al. in prep)

Deleted: (Hatta et al. in prep)

553 3.5 Modeling sensitivity experiments

555 The control model run agreed well with the data over a number of different depth strata (Fig. 8).
 556 In the surface layer (0-50m), the model output was most consistent with the observations (Fig.
 557 8A), although in general, the model tends to produce maximum levels of dCo that underestimate
 558 the highest dCo concentrations observed. Part of this is likely due to the fact that the model is
 559 comparing annual mean model output against synoptic scale in-situ observations. However, the
 560 model may underestimate sources of dCo in the Arctic. Below 50 m, there is also good
 561 agreement with observations (Fig. 8B), with the model capturing the much lower dCo

Deleted: Overall, t

Deleted: s

Deleted: i

Deleted: we are

Deleted:

Deleted: also be

Deleted: ing

characteristic of these waters and in particular the contrast between our data in the Arctic and other data from the North Atlantic (Dulaquais et al., 2014). In the deepest layers (Fig. 8C and D), the model again is able to reproduce the decline in dCo to ~ 60 pmol L⁻¹ and the consistency between the deep Arctic and North Atlantic.

In order to capture the major processes contributing to the modeled dCo sources and sinks, the proportion of the dCo signal in two distinct depth horizons was further investigated using a set of sensitivity experiments. In the 0-50 m depth range (Fig. 9), rivers in the model were shown to have no large scale impact on the Arctic-wide dCo signal (Fig. 9A), while removing sediment margin sources reduced dCo by over 80%, (Fig. 9B). Enhanced sediment Co supply under low oxygen also had no impact in this region. Similarly, modulating the effect of oxygen on Co scavenging had little impact in the Arctic (Fig. 9C). It was notable that in sensitivity experiments where bacterial biomass on scavenging was kept constant (e.g. by eliminating the effect of bacterial biomass on scavenging) the dCo concentrations were reduced by over 60% in surface waters in some regions, indicating that lower rates of scavenging were also contributing to the high concentrations of dCo in the surface ocean (Fig. 9D). Thus, our model experiments suggest that the high levels of dCo in the Arctic surface waters are due to high supply from sediments, combined with reduced scavenging rates due to lower metabolic activity of Mn-oxidizing bacteria due to the colder temperatures. In the 700-800 m depth horizon, we similarly found that changing sediment supply was more important than rivers (Fig. 10A and B), but that the effect of sediments was reduced at these depths compared to the surface. Equally, retardation of Co scavenging under low oxygen had a minor role in the ocean interior (Fig. 10C), with bacterial biomass again having a significant effect on the dCo signal (Fig. 10D). Thus, in contrast with the surface, we find that in the 700-800 m stratum there is a roughly equal role played by sediment Co supply and low rates of Co removal by Mn-oxidizing bacteria in maintaining the dCo concentrations.

4. Discussion

4.1 Quantifying external sources of cobalt to the Arctic Ocean

The coherence of the dCo and LCo distributions with that of dMn, along with evidence from the model output, suggest that shelf sediments are one of the primary sources of Co in the Canadian sector of the Arctic Ocean (Fig. 5, 9). Mn is known to be an excellent tracer of sediment input due to the high solubility of reduced Mn emanating from anoxic sediments (Johnson et al., 1992; März et al., 2011; McManus et al., 2012; Noble et al., 2012). By using the dMn concentrations as a tracer for shelf input, we can quantify the proportion of the variance in the dCo and LCo observations that are explained by this shelf proxy. Linear regressions between dCo or LCo distributions and dMn in the upper 200 m across all of the stations explains 73% and 79% of the variance in the dCo and LCo concentrations, respectively (Fig. 11A; $p < 0.05$). This trend is driven primarily by the data in the upper 50 m. The variance explained decreases however, if only the shelf stations (stations 2-10, 57-66) are included in the analysis (data not shown), suggesting that some process other than shelf inputs couples the dMn and Co distributions within the basin. The amount of the variance in the Co distributions that is explained by shelf inputs as indicated by dMn is slightly less than that observed in the model (Fig. 9B), though both agree that shelf inputs are the dominant source.

Deleted: explored

Deleted: The strong effect of

Deleted: sediment Co supply in the model is largely driven by the large shelf area in the Arctic.

Deleted: In contrast to the eastern tropical Pacific oxygen minimum zone where low oxygen concentrations contributed significantly to the source of dCo (Tagliabue et al., 2018) due to reductive dissolution of sedimentary Mn-oxides (Hawco et al., 2016), enhanced sediment Co supply under low oxygen had no impact in the Arctic, due to higher levels of oxygen typical of this basin.

Deleted: also

Deleted: keeping bacteria scavenging constant (e.g. eliminating the effect of changes in bacterial biomass on scavenging) reduced dCo at the surface by over 60% in some places, indicating that lower rates of scavenging was also contributing to the high rates of dCo in the surface ocean (Fig. 9D).

Deleted: ary

Deleted: supply

Deleted: with a secondary role played by reduced scavenging due to low rates of activity associated with Mn-oxidizing bacteria due to colder temperatures.

Deleted: i

Deleted: i

Deleted: i

Deleted: s

Deleted: interior

Deleted: signal

Deleted: These results are different to similar assessments in the southern equatorial Pacific where the lower oxygen levels typical of this region led to an enhanced role for sediment supply linked to low oxygen and reduced Co scavenging under low water column oxygen in driving high levels of dCo (Tagliabue et al., 2018).

Deleted: the extensive shelf sediments in the Arctic are the dominant source of Co in the Canadian section of the Arctic Ocean (Fig. 5, 9).

Deleted: reducing

Deleted: for shelf input

665 The modeling results suggest that nearly all of the dCo in the upper 50 m can be accounted for
 666 by a combination of a sediment source and diminished scavenging **in the Arctic relative to other**
 667 **ocean basins** (Fig. 9B and D; (Tagliabue et al., 2018)). However, the observations suggest that
 668 20-30% of the variance cannot be explained by a shelf source alone. If the dCo and LCo is
 669 examined against salinity for all stations **from GN01** in the upper 200 m, then salinity can
 670 explain 24% and 28% of the variance for dCo and LCo, respectively (data not shown). This
 671 relationship is improved if only the stations in the central Arctic basin are included (stations 30-
 672 43), and then salinity explains 47% of the dCo and 57% of the LCo distributions (Fig. 11B). The
 673 coherence of dCo and LCo with salinity across the dataset, and particularly in this region,
 674 appears to be due to a contribution of low salinity water from rivers, rather than from sea ice
 675 melt (Fig. 12C), as no relationship was observed with the fraction of sea ice melt determined
 676 from $\delta^{18}\text{O}$ isotopic measurements of seawater (Bauch et al., 2005; Cooper et al., 1997, 2005;
 677 Newton et al., 2013). Instead, the relationship with salinity is driven by freshwater inputs from
 678 rivers, as a strong relationship is observed with the fraction of meteoric water (Fig. 12D). These
 679 stations correspond to a region of anomalously high dFe and DOC concentrations (Charette et
 680 al., 2020), interpreted to be indicative of river inputs carried across the basin in the Transpolar
 681 Drift (TPD) (Gascard et al., 2008; Klunder et al., 2012; Middag et al., 2011; Wheeler et al.,
 682 1997). This is supported by measurements of ^{228}Ra , which track shelf inputs throughout the
 683 Arctic (Kipp et al., 2018; van der Loeff et al., 2018). A similar relationship was also observed
 684 with salinity in the North Atlantic, supporting the role of rivers as a source of dCo (Dulaquais et
 685 al., 2014a; Noble et al., 2016; Saito and Moffett, 2001). In our model sensitivity experiments, we
 686 found a small effect of rivers on dCo (Fig. 9A, 10A), and the Co/N river endmember in the
 687 model was similar to that measured by the Arctic Great Rivers Observatory (Holmes et al.,
 688 2018). It appears that the data suggest a larger role for rivers than what is captured by the model,
 689 which could imply that gross riverine fluxes are underestimated by our model. However it is
 690 difficult to disentangle riverine processes from other processes happening on the shelf like
 691 groundwater inputs (Charette et al., 2020). It is possible that there is some mixing of river and
 692 sediment dCo occurring in the coastal zone or that our global scale model is not able to properly
 693 account for the physical transport of fluvial signals into the open basin.

695 The presence of such high concentrations of trace elements and isotopes at the North Pole was
 696 surprising, yet several tracers indicate that this is an area significantly influenced by river and
 697 shelf input from the surrounding continents (Charette et al., 2020; Colombo et al., 2020; Kipp et
 698 al., 2018; van der Loeff et al., 2018). The elevated concentrations of dCo at great distances from
 699 the continental shelf is also likely partially due to the enhanced organic complexation of dCo in
 700 TPD waters. Averaged over the entire dataset dCo is $79 \pm 13\%$ organically complexed ($21 \pm 13\%$
 701 labile) in the upper 200 m of the water column. However, at TPD influenced stations (stations
 702 29-34; Charette et al., 2020), dCo is $92 \pm 6\%$ organically complexed, significantly higher than in
 703 the rest of the transect (*paired sample t-test*, $p < 0.05$). This suggests that elevated concentrations
 704 of DOC from Arctic rivers entrained in the TPD or ligands produced in-situ may play a role in
 705 stabilizing a portion of the dCo pool during transport towards the North Pole, **as has been**
 706 **observed for other metals such as dFe (Slagter et al., 2017, 2019) and dissolved copper (Nixon et**
 707 **al., 2019).** Although the exact character of the organic dCo-binding ligands in seawater are
 708 unknown, in the Arctic it is likely that humic-like substances contribute some portion of the
 709 organic complexation observed, due to the presence of elevated colored **DOM** (CDOM) in the

Deleted: inferences from

Deleted: in the transect

Deleted: (Jensen et al., in prep, D. Hansell, pers. comm.)

Field Code Changed

Formatted: Swedish

Formatted: Swedish

Deleted: due to interactions between the sediment-water exchange processes

Deleted: (Saito and Moffett, 2001)

Deleted: and

Deleted: s

Deleted: in review

Deleted: (Kipp et al., 2018; van der Loeff et al., 2018).

Formatted: Swedish

Formatted: Swedish

Formatted: Swedish

Deleted: in review

Deleted: dissolved organic matter

TPD (Wheeler et al., 1997), consistent with the presence of humic substances (Del Vecchio and Blough, 2004). Despite the presence of humic substances, it seems somewhat unlikely that humics account for all of the ligands complexing dCo in this region. Our analytical method distinguishes organically-bound Co as the fraction of total dCo that is more strongly complexed than our competing ligand (DMG). The complexation of humic and fulvic-like substances with Co has been shown to be much weaker than the Co(DMG)₂ complex ($\log K_{Co(HS)}^{cond} \sim 8$ versus $\log K_{Co(DMG)_2}^{cond} = 11.5 \pm 0.3$; Yang and Van Den Berg, 2009). Ligands similar to those suspected to complex Co in open ocean waters of the Atlantic or Pacific could be responsible for Co stabilization in the TPD waters (Saito and Moffett, 2001). These ligands are presumed to have functional groups similar to cobalamin (vitamin B₁₂), with a Co atom tightly bound inside a corrin ring. Cyanobacteria and some archaea are known cobalamin producers (Bertrand et al., 2007; Doxey et al., 2015; Heal, 2018; Heal et al., 2017; Lionheart, 2017) and both are found in the Arctic (archaea; Cottrell and Kirchman, 2009; cyanobacteria; Waleron et al., 2007; Zakhia et al., 2008), although in very low abundance. The nature of the organic molecules binding dCo in this region will be interesting to explore further in future studies.

Overall, both the modeling results and observations agree that the dominant source of Co in the Arctic is from the extensive shelf sediments surrounding the Arctic Ocean, with additional contributions from Arctic rivers. The observations however, show that sources vary in importance in space, with sediment sources clearly dominating in stations close to the shelf, and river sources dominating in the central Arctic basin through the influence of the TPD. The interaction between rivers and shelves requires further inquiry, as the shelf sediments might behave as “capacitor” for dCo, accumulating Co from rivers and sinking organic matter and then releasing Co to the overlying water during reductive dissolution in the sediments (Bruland et al., 2001; Chase et al., 2007). Although the mechanism is uncertain, it is clear that the riverine source dominates the distribution observed near the North Pole where dCo and LCo concentrations remain high despite the distance from land, and that organic complexation likely plays a role in the distal transport of this dCo (Charette et al., 2020).

4.2 Cobalt scavenging and internal cycling

A striking feature of the dCo and LCo dataset is the vertical transition in the water column from high to low Co concentrations throughout the deep Arctic (Fig. 5). The question remains whether or not 1) this elevated dCo is scavenged at a shallow depth horizon, or 2) if the high dCo concentrations in the surface layer (< 200 m) are simply physically isolated from deeper water masses, or a combination of the two. This would suggest that the Atlantic water characteristic of the deep Arctic doesn't mix with the modified surface Arctic water containing high concentrations of Co. We examined both hypotheses within a modeling framework and compared this to the observations. In the model, the dCo is scavenged primarily in the upper 50 m with almost no scavenging below 200 m (data not shown). The dCo scavenging in the model is primarily controlled by Mn-oxidizing bacteria, which have a strong temperature dependence in the model (Tebo et al., 2004). The cold temperatures in the majority of the Arctic prevent enhanced scavenging of dCo by this mechanism compared to other basins (Hawco et al., 2018; Saito et al., 2017; Tagliabue et al., 2018). However, relatively warmer temperatures on the shallow shelves suggest that scavenging is enhanced in this region (Fig. 4), and the coherence of the pCo and pMn peaks in the upper 200-250 m (Fig. 7) support this mechanism of upper ocean

Deleted: Whether or not shelf sediments act as a capacitor, storing and then releasing Co to overlying water, for terrestrially derived riverine sources or for Co delivered to sediments in sinking marine organic matter remains unknown. It is clear however, that the riverine source dominates the distribution observed near the North Pole where dCo and LCo concentrations remain high despite the distance from land, and that organic complexation likely plays a role in the distal transport of this dCo (Charette et al., in review). ¶

Deleted: in the Arctic

scavenging. Evidence from ^{234}Th data shows very little particulate organic carbon (POC) flux in the upper water column along this transect, however strong lateral transport from the shelves to the basin was observed (Black et al. 2018). This lateral transport was observed both in the upper water column and at depth, suggesting fast-moving currents through the deep canyons may be significant in transporting material from the shelf into the basin (Black et al. 2018). It is possible that additional scavenging of Co may occur along this flow path. Some of the profiles observed in the deep basin also show evidence for deeper ocean scavenging in the Atlantic water (e.g. Fig. 4E, H, P).

Additional insights on Co scavenging in this basin can be observed by exploring the dCo:phosphate (P) ratios ($\text{pmol L}^{-1}:\mu\text{mol L}^{-1}$) along the transect (Fig. 13). The relationship between dCo and P in the Arctic water column yields insights into biological uptake and regeneration processes acting on the dCo inventory, as well as scavenging. An analysis completed by Saito et al. (2017) showed that positive slopes in the dCo:P relationship were indicative of regeneration, while negative slopes were indicative of biological uptake or scavenging (Saito et al., 2017). The high dCo in the Arctic yields a unique dCo:P relationship compared to the North Atlantic (Fig. 13A; Saito et al., 2017). When dCo:P slopes ($r^2 > 0.6$) are binned according whether they are positive (Fig. 13B) or negative (Fig. 13C) and then plotted with depth (Fig. 13D), a few patterns are apparent. Positive dCo:P slopes are observed largely within a confined depth layer in the PHW (Fig. 13D). This is not surprising, given that deep Pacific waters carry a strong regeneration signal. However, at most other depths the dCo:P slopes are negative, showing that scavenging is occurring to some extent throughout the water column (Fig. 13D). With one exception, the magnitude of the negative dCo:P slopes are greater in the upper water column, supporting the model results and our interpretations of the pCo profiles that most of the scavenging occurs in the upper water column but also continues to occur throughout the deep Arctic.

This evidence, combined with the coinciding maxima observed in pCo and pMn, suggest that scavenging occurs in the upper water column, but that additional scavenging continues to occur in deeper waters. The elevated pCo concentrations in the deep Arctic compared to other regions (Lee et al., 2018) suggest that scavenging over long timescales continue to add to the pCo pool. The strong stratification in the Arctic likely prevents high concentrations of dCo from mixing between the modified surface waters, the PHW, and the deep Atlantic water (Steele et al., 2004). Thus, it is likely a combination of limited upper ocean scavenging, and strong stratification between water masses, that keeps the elevated dCo and LCo confined to the surface waters in Arctic, yielding the intense scavenged-like profile of Co in this region compared to other basins (Fig. 3).

4.3 Increases in Co inventories over time in the Canadian sector of the Arctic Ocean

Samples collected on the shelf in the Beaufort Sea in 2009 in proximity to the U.S. GEOTRACES transect in 2015 (Fig. 1) had significantly lower dCo (paired *t*-test, $p < 0.05$) than shelf samples from 2015 (Fig. 14). Shelf samples for dCo from 2015 were approximately four times higher than the dCo and approximately eight times higher in LCo than in 2009 (Fig. 14C). The maximum dCo concentration measured in 2009 was 301 pmol L^{-1} , while in 2015 it was 1852 pmol L^{-1} . The dCo and LCo concentrations below 150 m agreed very well however, between the

Deleted: (to no)

Deleted: strata

Deleted: in the water column

Deleted: a significant amount of

Deleted: below these dep

Deleted: this

Deleted: This mechanism likely prevents high concentrations of dCo to penetrate below the shallow modified Arctic surface water. However, it is clear that there is very little mixing between the modified surface waters, the PHW, and the deep Atlantic water in the Arctic (Steele et al., 2004). Thus, it is likely a combination of upper ocean scavenging, and little mixing between water masses, that keeps the elevated dCo and LCo confined to the surface waters in Arctic, yielding the intense scavenged-like profile of Co in this region compared to other basins (Fig. 3).

Deleted: 3.5

two years (Fig. 14A, B). Several factors could account for the higher dCo and LCo observed in 2015 compared to 2009. The Co samples from 2009 were initially unfiltered, and were not stored with gas-absorbing satchels like the samples from 2015. Recently, loss of dCo has been observed in the presence of oxygen during storage, however this loss was most pronounced for samples in low oxygen regions (Noble, 2012). The mechanism of the dCo loss is unknown and is difficult to quantify from these samples, however the waters are well oxygenated in this region (Fig. 2B) and thus the loss due to storage was likely minimal. However, we cannot say for certain how much of the observed increase in dCo over time is due to a storage artifact. Previous work has shown a maximum loss of dCo of 40% after 5 months of storage (Noble, 2012). If we consider that 40% of the dCo could have been lost in the samples collected from 2009, the data from 2015 still show an increase in dCo of approximately 400%. Thus, although we cannot quantify with certainty the percent increase in dCo over time in the Canadian sector of the Arctic, it is likely that a large increase in dCo was observed.

Deleted: unfiltered

Deleted:

Deleted:

Deleted: that it is still significant.

The increase in dCo over time in the Arctic is interesting, and has been documented for other tracers in the Arctic. Kipp et al. (2018) and van der Loeff et al. (2018) noted that ^{228}Ra has increased over time in the central Arctic. They suggest that increases in shelf and/or river inputs from thawing permafrost are the source of this elevated ^{228}Ra (Kipp et al., 2018; van der Loeff et al., 2018). A similar mechanism is likely increasing metal inventories over time on Arctic shelves. The majority of the variance (~70%) in dCo in the upper 100 m on the U.S. GEOTRACES transect could be explained by a shelf source, and the remainder was likely associated with river inputs (Fig. 11). If these sources are similar to the sources of dCo in 2009, then an increase in either a shelf or river flux could be responsible for the dramatic increase in dCo over time. While there is not enough data to state whether the river dCo flux has in fact changed over time in the Arctic and the observed changes could be due to seasonal or interannual variability, several other studies have documented an increase in river discharge due to increases in permafrost melt over time (Doxaran et al., 2015; Drake et al., 2018; Kipp et al., 2018; van der Loeff et al., 2018; Tank et al., 2016; Toohey et al., 2016). The increase in river discharge has the potential to considerably increase trace metal inventories in the future Arctic Ocean, perhaps particularly for those metals that are strongly organically complexed, thus protecting against scavenging in the estuarine mixing zone (Bundy et al., 2015). We recognize these two Arctic dCo datasets are limited in temporal coverage and have methodological differences; however, we felt a responsibility to transparently present these observations of dCo increases in the Arctic Ocean to raise community awareness of this potential environmental change. These increases in metals over time may have implications for metal stoichiometries and phytoplankton growth in a changing Arctic Ocean.

Deleted: There is not enough data to state whether the river dCo flux has changed over time in the Arctic, however several studies have documented an increase in river discharge over time due to increases in permafrost melt (Doxaran et al., 2015; Drake et al., 2018; Kipp et al., 2018; van der Loeff et al., 2018; Tank et al., 2016; Toohey et al., 2016).

Formatted: Swedish

Formatted: Swedish

Deleted: These increases in metals over time will have implications for metal stoichiometries and phytoplankton growth in a changing Arctic Ocean.

4.4 Implications of the Arctic as a net source of Co to the North Atlantic Ocean

The concentrations of dCo and LCo in this region of the Arctic are some of the highest that have been observed thus far in the ocean. In some cases, the dCo was almost ten times higher than in the low oxygen region of the Eastern Pacific (Hawco et al., 2016). Although the Arctic is considered to be a macronutrient poor system, in contrast to other oligotrophic regions the Arctic is quite enriched in micronutrients (Charette et al., 2020; Colombo et al., 2020; Jensen et al., 2019; Marsay et al., 2018; Slagter et al., 2017). These distinct micronutrient ratios may have

Deleted: concentrations

Deleted: (Jensen et al., 2019; Jensen et al., in prep)

Formatted: Swedish

904 implications for Arctic phytoplankton communities, as well as communities in the North Atlantic
905 that are influenced by inputs from the Arctic.

906
907 Arctic waters are thought to primarily exit the basin and impact the North Atlantic via the
908 Canadian archipelago and the Fram and Davis Straits (Talley, 2008). The organic complexation
909 and stabilization as well as the high concentrations of dCo suggest that some of this dCo might
910 exit the Arctic and impact nutrient distributions in the North Atlantic. Noble et al. (2016) noted a
911 plume of elevated dCo in the western portion of the U.S. GEOTRACES North Atlantic (GA03)
912 transect that did not correspond with a signature from reducing sediments as on the North
913 Atlantic eastern boundary. Noble et al. (2016) postulated that high dCo in Labrador Seawater
914 (LSW) was the source of this signal, due to the presence of a corresponding signature of low
915 silica that is characteristic of this water mass. The authors noted that the anomalously high dCo
916 could be from elevated dCo in Arctic waters, or due to high dCo on the shelf that is picked up
917 along the flow path of the LSW, or a combination of the two (Dulaquais et al., 2014a; Noble et
918 al., 2016). This observation was also noted by Dulaquais et al. (2014) in the GEOTRACES
919 GA02 section (Dulaquais et al., 2014a, 2014b). Our data suggests that likely a combination of
920 the high dCo observed in this study and additional Co entrained on the shelf in the Labrador Sea
921 contribute to that signal, and when observed in temperature and salinity space the data supports
922 this hypothesis (Fig. 15). The Arctic source waters that contribute to the formation of LSW have
923 a low salinity signature, and are likely significantly modified as they exit the Canadian
924 archipelago, Fram Strait and Davis Straits (Yashayaev and Lodor, 2017). From this data we
925 cannot quantitatively connect the elevated dCo and LCo observed in the Arctic source waters to
926 the LSW seen in the western Atlantic (Dulaquais et al., 2014a; Noble et al., 2016), given the
927 complex history (e.g. transformation, mixing) of source waters in the Labrador Sea region (Le
928 Bras et al., 2017). However it is apparent that the low salinity Arctic waters contain high Co
929 (Fig. 15), which given the advective pathways of these water masses from the Arctic, suggests
930 that they may act as a source of Co to lower latitude waters. Interestingly, the high dCo in the
931 Arctic has a distinct LCo/dCo signature compared to that observed in the western North Atlantic
932 (Fig. 15A). Due to the significant impact that Arctic shelves and rivers have on the dCo signature
933 observed in this study, it is likely that additional Co may be added to these waters as they pass
934 through the Canadian archipelago. The fate of these waters and their Co as they exit via the Fram
935 and Davis Straits is unknown. Constraining these Arctic endmembers and how they contribute to
936 dCo distributions in the North Atlantic deserves further attention, as it has interesting
937 implications for nutrient resource ratios for North Atlantic phytoplankton communities.

938
939 The possibility that elevated micronutrient concentrations from the Arctic are being exported to
940 the North Atlantic could have implications for phytoplankton nutrient utilization and community
941 composition. The dCo and dZn for example, which can be interchanged within carbonic
942 anhydrase in some eukaryotes (Lane and Morel, 2000; Sunda and Huntsman, 1995; Yee and
943 Morel, 1996), are elevated in the Arctic (Jensen et al., 2019) compared to the North Atlantic and
944 South Pacific (Fig. 16A, B (Schlitzer et al., 2018)). The higher concentrations of both metals
945 results in a dCo/dZn ratio that is quite similar to that observed in the North Atlantic, however the
946 range in this ratio is large (Fig. 16C). Small changes in the sources of each of these metals could
947 manifest as big impacts on the ratio of these micronutrients in surface waters, which laboratory
948 studies have shown to have significant effects on growth (Hawco and Saito, 2018; Kellogg et al.,
949 2020; Sunda and Huntsman, 1995). The cellular Co/Zn ratios are also slightly higher in the

Deleted: (Noble et al., 2016)

Deleted: Additional LCo is likely entrained in this water mass as the surface Arctic water moves through the Canadian archipelago.

Deleted: interesting

Deleted: D

Deleted: However, the shift in these micronutrient ratios may not impact the resulting phytoplankton quotas (Figure 16D).

Arctic compared to the North Atlantic but span a similar range (Twining et al. in prep, Figure 16D). However, if river inputs continue to increase with an increase in permafrost thawing in the warming Arctic (Jorgenson et al., 2006) and similar increases in dCo are observed over time as seen in this work, then the inventory of dCo in the Arctic may begin to influence the North Atlantic to a greater extent. These increases in metal sources may disproportionately affect Co compared to Zn, whose primary source was found to be from a regeneration signal on the shelf rather than from river input (Jensen et al., 2019), and whose total inventory is small compared to Zn. For example, diatoms that have enhanced growth rates when metabolically substituting Co for Zn may be favored in surface waters with higher dCo/dZn ratios (Kellogg et al., 2020), although there is no experimental data to our knowledge examining the influence of Zn and Co on Arctic phytoplankton. Understanding how future changes in metal sources in the Arctic may impact the North Atlantic or shifts in phytoplankton community structure will be important to constrain.

5. Conclusions

The unique dissolved and labile Co distributions observed in the Arctic compared to other open ocean basins have potential implications for future changes in micronutrients in the warming Arctic Ocean. Sediment and river inputs to the Arctic appear to be the dominant mechanisms for the input of dCo to the Arctic, and these elevated signals persist over a broad area of the western Arctic far from their source regions. In part, this appears to be due to relatively slow scavenging of Co in the Arctic, highlighting the impact of lower temperatures and slower kinetics of Mn-oxide formation in this basin. The dCo in the Arctic is also strongly organically-complexed, which may also prevent scavenging and lead to the persistently high concentrations observed in surface waters. Notably, Co was also shown to be increasing over time on the shelf in the Canadian Arctic, likely due to increases in river inputs from thawing permafrost, consistent with other Arctic tracers. The increase in the inventory of dCo over time in the Arctic may have downstream impacts on dCo/dZn ratios in North Atlantic waters, as the dCo inventory will be disproportionately magnified relative to dZn with additional future increases from Arctic rivers. Higher dCo/dZn ratios in the Arctic and North Atlantic may also favor organisms that have elevated growth rates if Co is metabolically substituted for Zn. These ecological impacts are likely to become increasingly important in the future, with increased warming and changes to Co sources in the Arctic basin.

6. Author contributions

RMB analyzed the samples and wrote the manuscript. MRC developed the data processing code and helped write the manuscript. MAS designed the study and helped write the manuscript. AT, NJH, PLM, BST, MH, AN, SGJ, and JTC contributed data and helped write the manuscript.

7. Data availability

The metadata for this manuscript are available through BCO-DMO for GN01 (<https://www.bco-dmo.org/project/638812>) and through BODC for GIPY14 (<https://www.bodc.ac.uk/geotraces/data/inventories/0903/>). The dissolved and labile cobalt data for GN01 specifically is available at <https://www.bco-dmo.org/dataset/722472>.

8. Acknowledgements

Deleted: Despite quite different total concentrations of dCo and dZn in the Arctic compared to the North Atlantic for example, the measured quotas are quite similar (Twining et al. in prep, Figure 16D).

Deleted: total metal inventories in the Arctic may begin to influence the North Atlantic to a greater extent.

Deleted: These source changes may disproportionately affect Co compared to Zn, whose primary source was found to be from a regeneration signal on the shelf rather than from river input (Jensen et al., 2019), and whose total inventory is small compared to Zn. Understanding how future changes in metal sources in the Arctic may impact the North Atlantic or shifts in phytoplankton community structure will be important to constrain.

Deleted: The unique dissolved and labile Co distributions observed in the Arctic have noteworthy implications for Arctic ecosystems and for future changes in micronutrients in the warming Arctic. Sediment and river inputs to the Arctic appear to be the dominant mechanisms for the input of dCo to the Arctic, and these elevated signals persist over a broad area of the western Arctic far from their source regions. This appears, at least in part, to be due to the relatively slow scavenging of Co in this basin that is suggested from modeling outputs to be related to the low temperatures and slower kinetics of Mn-oxide formation. The majority of this scavenging appears to happen on the shelf with an advected signal of particulate Mn and Co appearing into the Arctic basin. Co was also shown in this work to be increasing over time on the shelf in the Canadian Arctic, possibly due to increases in river inputs from thawing permafrost, though this is difficult to constrain in the present dataset. Given the significant increase in Co over time in the Arctic and the modification of low-salinity Arctic waters as they exit the Arctic into the North Atlantic and the Labrador Sea, it is difficult to determine if there is a net flux of Co out of the Arctic and into the North Atlantic, however evidence in this work suggests that the distinct Co waters of the Arctic likely impact downstream micronutrient concentrations. These impacts are likely to become increasingly important in the future, with increased warming and changes to Co sources in the Arctic basin.

Deleted: data

1047 We would like to thank the captain and crew of the USGC *Healy*, Gabi Weiss and Simone Moos
1048 for sampling, and Dawn Moran, Noelle Held and Matt McIlvin for help with sample preparations
1049 and analyses, Dr. Ana Aguilar-Islas and Dr. Robert Rember for small boat and sea-ice hole
1050 operations, the Ocean Data Facility at Scripps Institution of Oceanography for macronutrient,
1051 oxygen, and salinity measurements, S. Rauschenberg for sample collection, and P. Schlosser, R.
1052 Newton, T. Koffman, and A. Pasqualini for water mass fraction data. This work was supported
1053 by NSF-OCE #1435056, 1736599 and 1924554 to M. Saito, as well as Woods Hole
1054 Oceanographic Institution Postdoctoral Scholar grant to R.M. Bundy and M.R. Cape. M. Hatta
1055 was supported by NSF-OCE #1439253. A. Tagliabue was supported by the European Research
1056 Council (ERC) under the European Union's Horizon 2020 research and innovation programme
1057 (Grant agreement No. 724289). BT was supported by NSF-OCE #1435862. PM was supported
1058 by NSF-OCE #1436019, and a portion of the work was completed at the NHMFL, which is
1059 supported by the NSF through DMR-1644779 and the State of Florida. J.T. Cullen was
1060 supported by the Natural Sciences and Engineering Research Council (NSERC) of Canada and
1061 an International Polar Year (IPY) Canada grant.

Deleted: We would like to thank the captain and crew of the USGC *Healy*, Gabi Weiss and Simone Moos for sampling, and Dawn Moran, Noelle Held and Matt McIlvin for help with sample preparations and analyses, Dr. Ana Aguilar-Islas and Dr. Robert Rember for small boat and sea-ice hole operations, the Ocean Data Facility at Scripps Institution of Oceanography for macronutrient, oxygen, and salinity measurements, S. Rauschenberg for sample collection, and P. Schlosser, R. Newton, T. Koffman, and A. Pasqualini for water mass fraction data. This work was supported by NSF-OCE #1435056 to M. Saito and S. John, as well as Woods Hole Oceanographic Institution Postdoctoral Scholar grant to R.M. Bundy and M.R. Cape. M. Hatta was supported by NSF-OCE #1439253. A. Tagliabue was supported by the European Research Council (ERC) under the European Union's Horizon 2020 research and innovation programme (Grant agreement No. 724289). PM and BT were supported by NSF-OCE #1435862 and PM was also supported by the National High Magnetic Field Laboratory (PLM). PLM is supported by the National Science Foundation through DMR-1644779 and the State of Florida. J.T. Cullen was supported by the Natural Sciences and Engineering Research Council (NSERC) of Canada and an International Polar Year (IPY) Canada grant.

Table 1: Average dCo concentrations from blank, internal standard, and consensus standard runs.

	n	dCo (pmol L⁻¹)	std dev
blank	29	2.5	0.7
internal standard	26	50.3	7.6
SAFe D1	3	47.9	2.1
SAFe D2	3	45.2	2.1
GSP	3	2.4	1.8
GSC	3	77.9	2.8

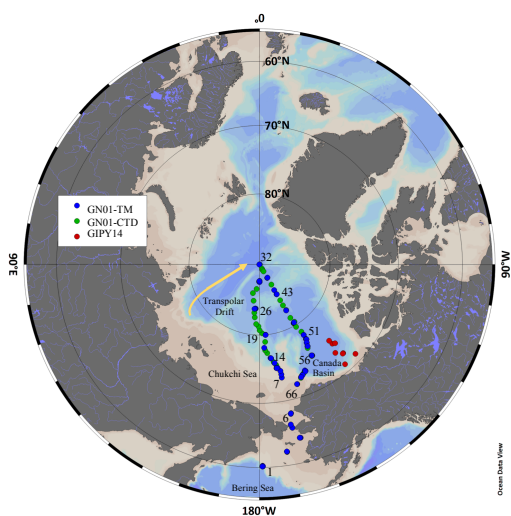
Table 2: Median, maximum and minimum concentrations of total dissolved (dCo) and labile cobalt (LCo) in samples with representative water masses and sources in the Arctic Ocean. Median concentrations were determined in each water mass type by using water masses that contained > 95% Atlantic water, > 95% Pacific water, > 10% meteoric water, and > 1.5% sea ice melt. Shelf stations were stations 2-10 and 60-66, MIZ stations 10-17 and 51-57 (< 30 m), and North Pole stations 27-36 (< 200 m). Ice hole samples were sampled from 1 and 5 m. The notation 'nd' means not determined.

	dCo (pmol L ⁻¹)	max	min	<i>n</i>	LCo (pmol L ⁻¹)	max	min	<i>n</i>
Atlantic	61.6	126.3	36.9	37	2.2	5.8	0.2	27
Pacific	269.6	687.3	64.1	41	45.8	133.8	2.5	35
Meteoric	266.1	497.2	64.1	27	77.5	139.8	11.6	25
Shelf	526.0	1852.1	25.9	30	148.0	578.7	6.1	30
MIZ	357.5	546.2	25.9	19	117.0	158.6	6.1	19
North Pole	139.8	280.2	64.2	14	10.3	22.0	1.5	14
sea ice melt	526.0	1021.5	207.3	3	151.1	233.0	48.8	3
ice hole	281.1	316.2	259.4	4	nd	nd	nd	4

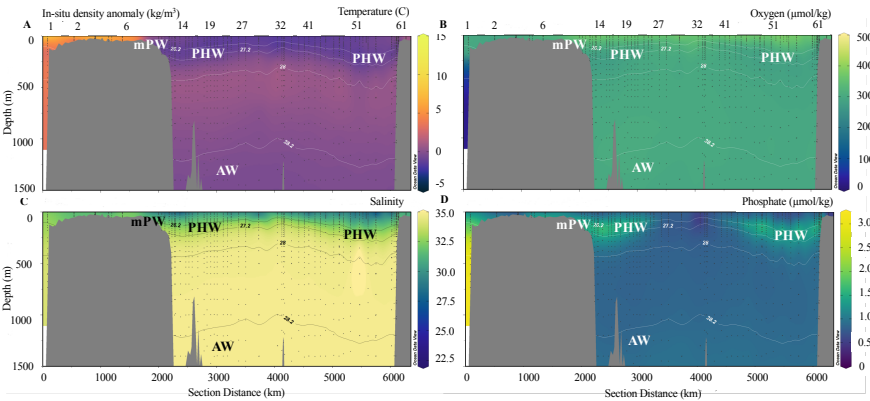
1086 **Figure Captions**
 1087 **Figure 1:** Standard CTD sampling stations (green) and trace metal rosette (TM) sampling
 1088 stations (blue) from the GN-01 expedition in 2015, and trace metal sampling locations from the
 1089 GIPY14 expedition in 2009 (red).
 1090 **Figure 2:** *In-situ* temperature (A), nitrate (B), salinity (C), phosphate (D), oxygen (E), and
 1091 silicate (F) with neutral density anomaly contours from the northern and southern legs of the
 1092 GN-01 transect as shown in Figure 1. Major water masses are labeled as modified Pacific Water
 1093 (mPW), Pacific Halocline Water (PHW) and Atlantic Water (AW).
 1094 **Figure 3:** Median dCo concentrations at specific depth intervals from the Arctic Ocean (this
 1095 study; red circles), Atlantic Ocean (blue triangles), and the Pacific Ocean (orange squares).
 1096 Shaded regions indicate the upper and lower quartiles of the data in each dataset.
 1097 **Figure 4:** Dissolved cobalt (dCo; black circles) and labile cobalt (LCo; open circles) from all
 1098 stations from the 2015 (A-Q) and 2009 (R) studies.
 1099 **Figure 5:** (A) dCo concentrations and (B) LCo concentrations in the Arctic Ocean.
 1100 **Figure 6:** The ratio of LCo (pmol L⁻¹) to total dCo (pmol L⁻¹) along the transect from south to
 1101 north in the upper 1000 m.
 1102 **Figure 7:** Particulate manganese (pMn; open circles) and particulate cobalt (pCo; x) from
 1103 several stations along the northern (A-D) and southern (E-H) legs of transect, with the same
 1104 station designations as in Figure 4.
 1105 **Figure 8:** Model output (colors) compared to observations (dots) from 0-50 m (A), 50-150 m
 1106 (B), 700-800 m (C) and 1500-2000 m (D).
 1107 **Figure 9:** (A) Model output of the proportion of the dCo signal from 0-50 m that is controlled by
 1108 (A) rivers, (B) sediment input, (C) oxygen concentrations, and (D) removal by Mn-oxidation
 1109 from Mn-oxidizing bacteria.
 1110 **Figure 10:** (A) Model output of the proportion of the dCo signal from 700-800 m that is
 1111 controlled by (A) rivers, (B) sediment input, (C) oxygen concentrations, and (D) removal by Mn-
 1112 oxidation from Mn-oxidizing bacteria.
 1113 **Figure 11:** dCo (closed circles) and LCo (open circles) in the upper 200 m plotted against (A)
 1114 dMn in shelf stations only (stations 2-10, 57-66), as well as (B) salinity from only the stations
 1115 influenced by the Transpolar Drift (stations 30-43).
 1116 **Figure 12:** dCo and LCo from select stations versus (A) the fraction of Atlantic water (F_{atl}; all
 1117 stations < 500 m), (B) the fraction of Pacific water (F_{pac}; all stations < 500 m), (C) fraction of sea
 1118 ice melt (F_{ice}; < 100 m and south of 84°N) and (D) the fraction of meteoric water (F_{met}; < 500 m
 1119 and north of 84°N).
 1120 **Figure 13:** (A) The dCo (pmol L⁻¹) compared to phosphate (dP; μmol L⁻¹) from the GN01
 1121 dataset. (B) 5-point two-way linear regression of positive dCo:P slopes ($r^2 > 0.6$). (C) 5-point
 1122 two-way linear regression of negative dCo:P slopes ($r^2 < -0.6$). (D) Depths where either a
 1123 positive (blue) or negative (red) dCo:P slope was identified in the GN01 dataset. Additional
 1124 details on the regression analysis can be found in Saito et al., (2017).
 1125 **Figure 14:** The dCo on the shelf measured in 2009 (GIPY14; black triangles) and 2015 (GN01;
 1126 blue circles) in the upper 3500 m (A) and upper 500 m (B). Average and dCo and LCo in the
 1127 upper 150 m from 2009 (grey) and 2015 (blue). Error bars represent the standard deviation and a
 1128 (*) denotes a significant difference.
 1129 **Figure 15:** (A) The ratio of LCo to dCo (colors) from this study and the western portion of the
 1130 GA03 North Atlantic transect (Noble et al., 2016) along with dCo concentrations (B) in
 1131 temperature-salinity space, with Labrador Sea Water (LSW) source waters (solid black box) and

signature in the Atlantic (dashed box) are highlighted. (C) Sampling region in this study and the stations used from Noble et al. (2016).
Figure 16: Median dCo concentrations (A), dissolved Zn concentrations (B) and dCo/dZn ratios (C) in the upper 200 m in the Arctic (this study), North Atlantic (Noble et al., 2016), and in the Southern Eastern Pacific (Hawco et al., 2016). (D) Co/Zn ratios in phytoplankton from the Arctic and North Atlantic (Twining et al., in prep). Whiskers represent the lower (25%) and upper (75%) quartiles.

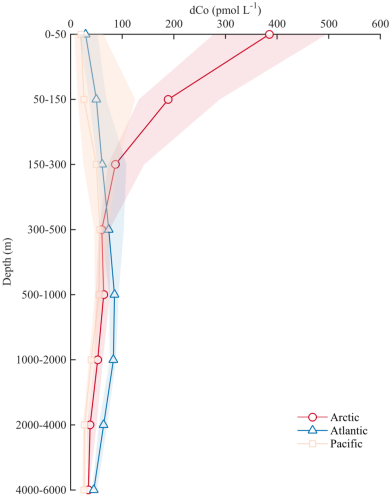
1139 **Figure 1.**



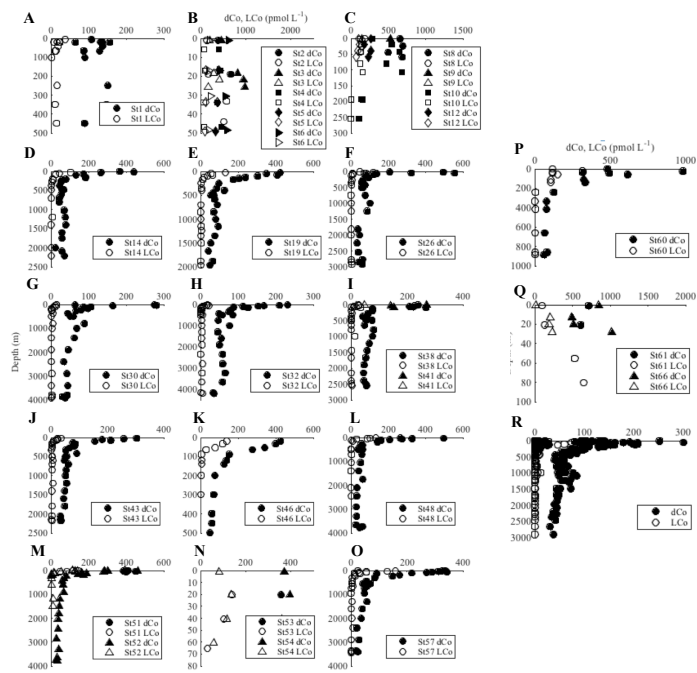
1140 **Figure 2.**



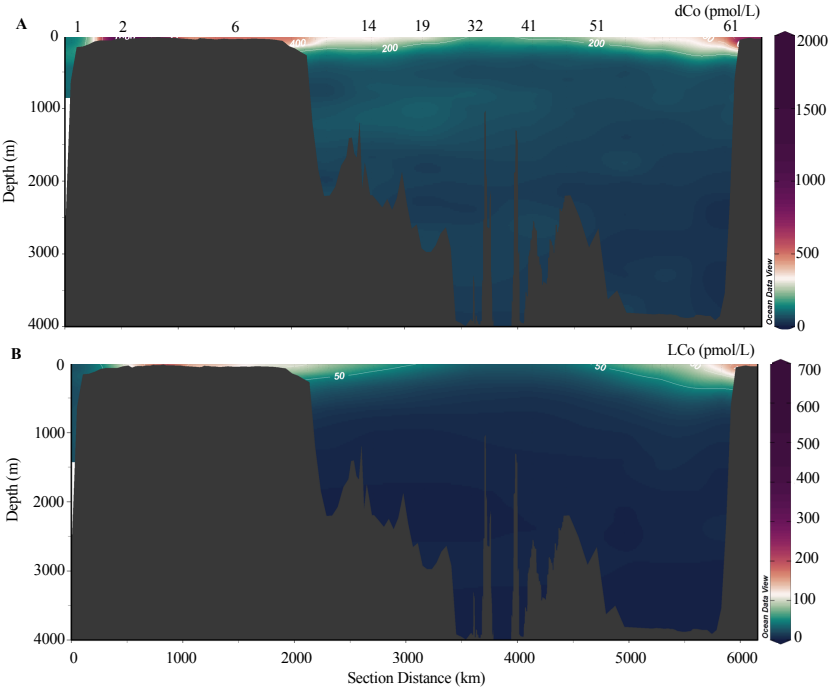
1141 **Figure 3.**



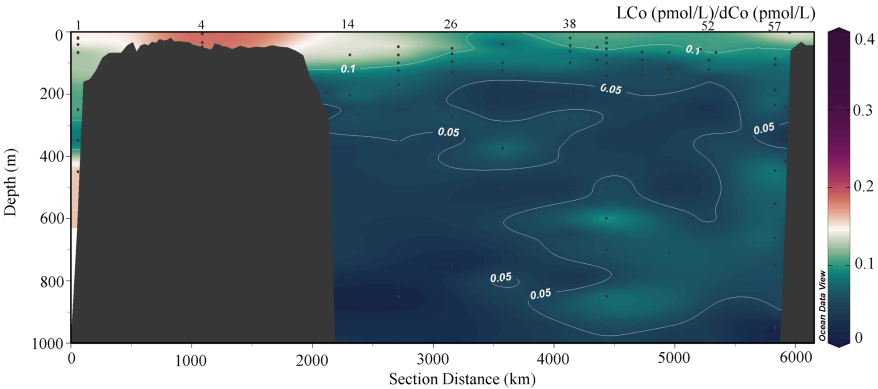
1142 **Figure 4.**



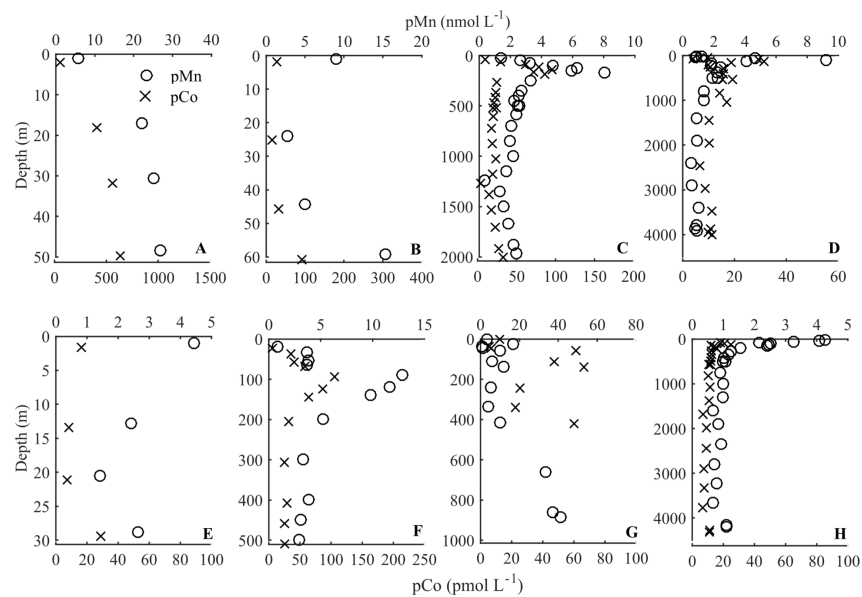
1143 **Figure 5.**

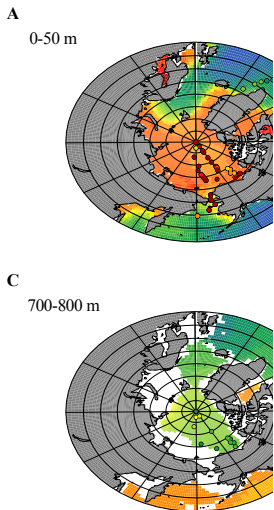
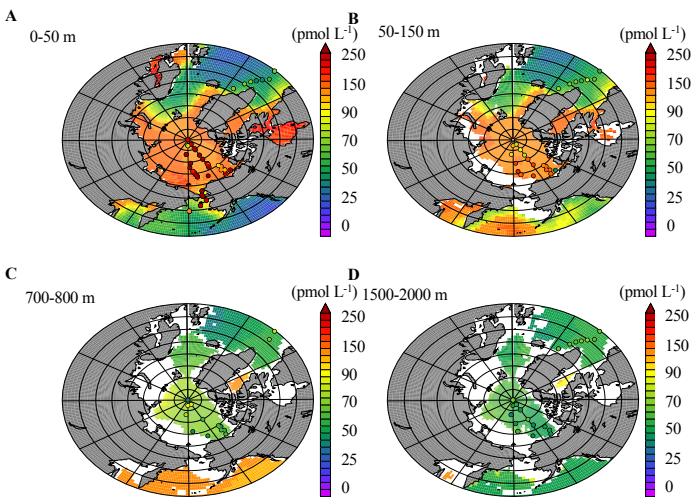


1144 **Figure 6.**

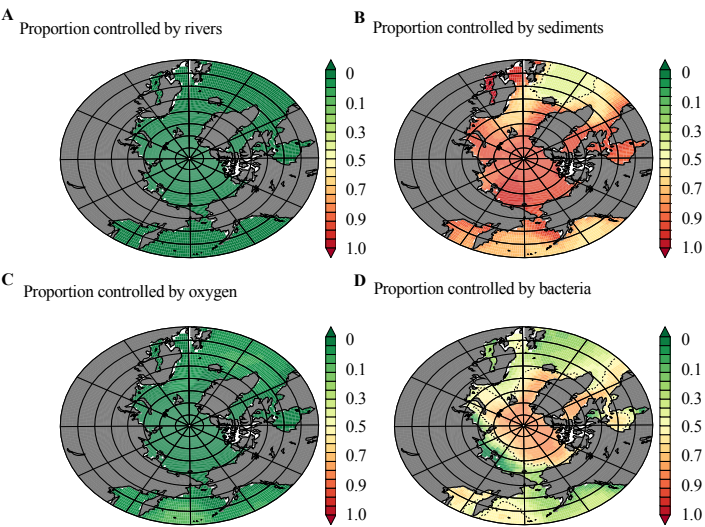


1145 **Figure 7.**

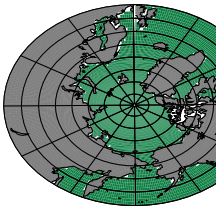




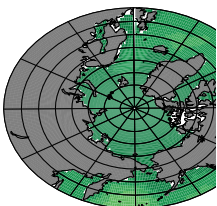
Deleted:



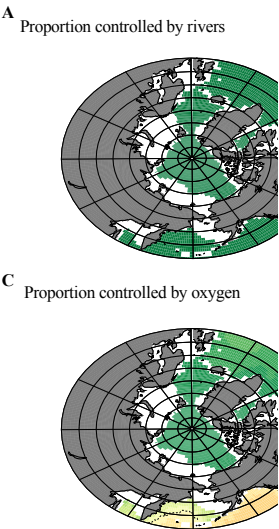
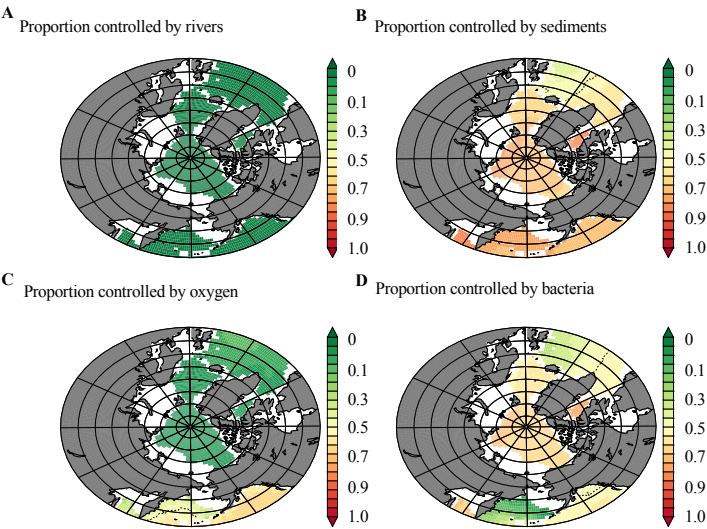
A Proportion controlled by rivers



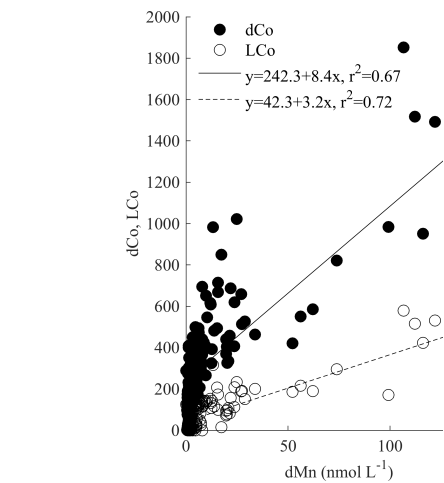
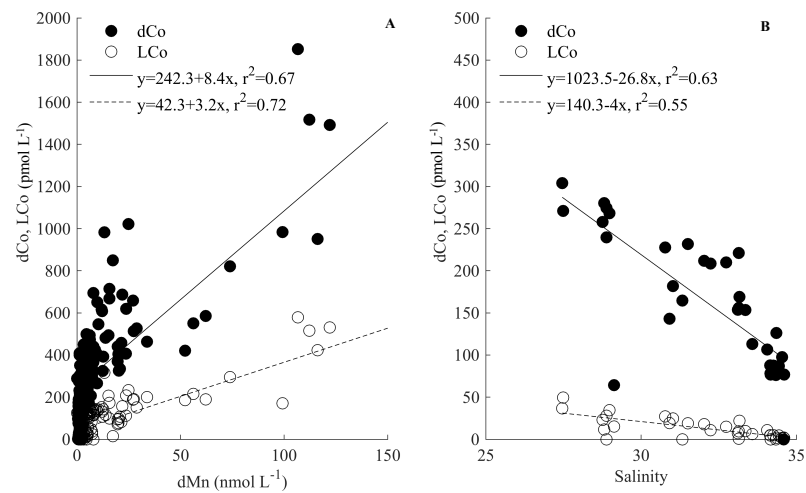
C Proportion controlled by oxygen



Deleted:

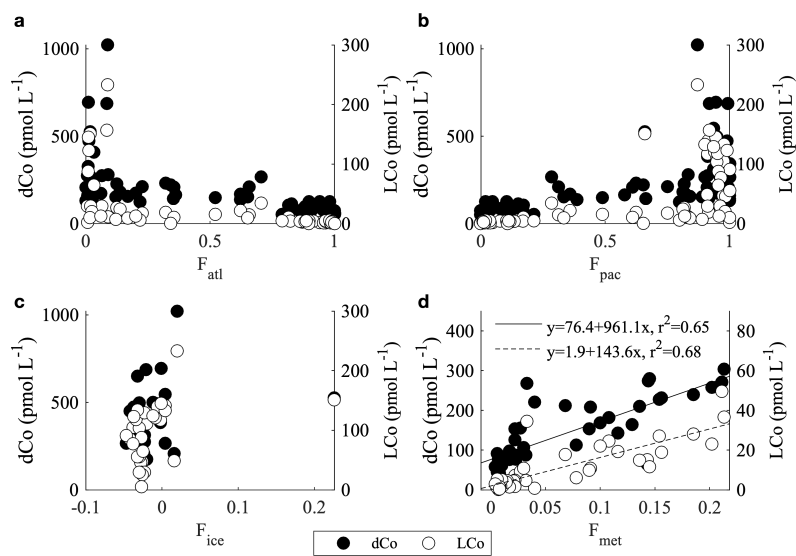


Deleted:

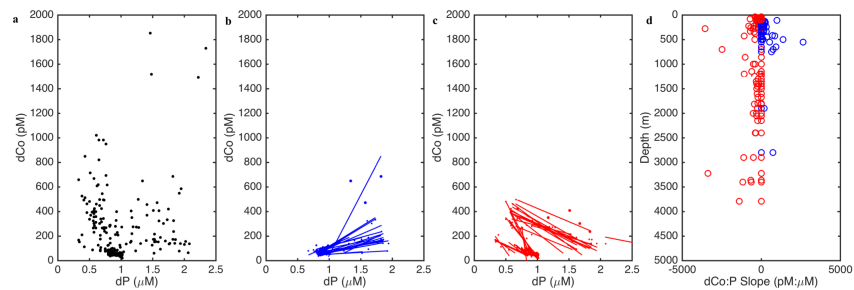


Deleted:

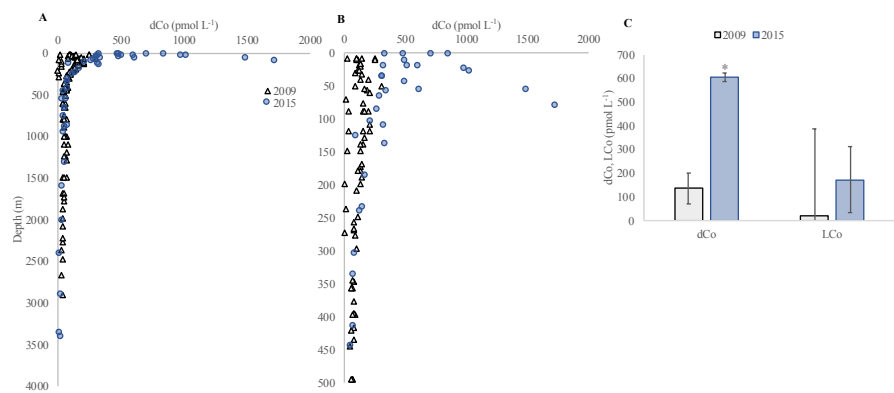
1150 **Figure 12.**



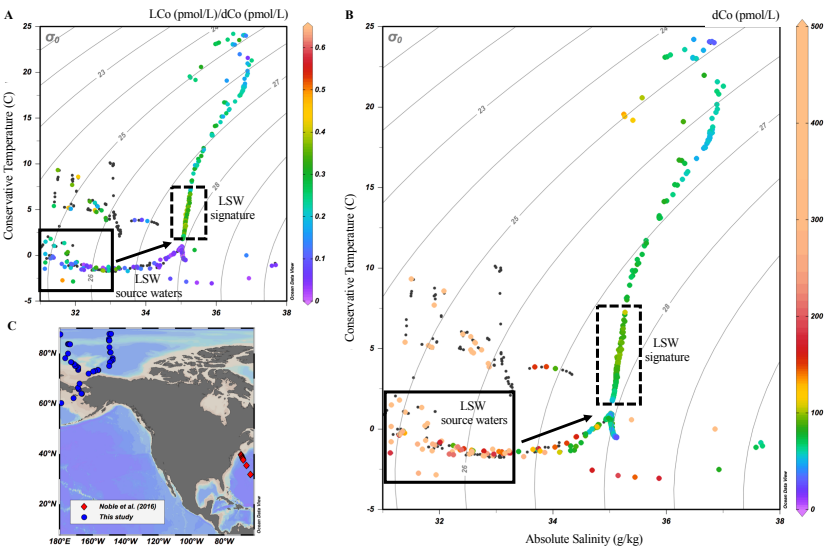
1151 **Figure 13.**

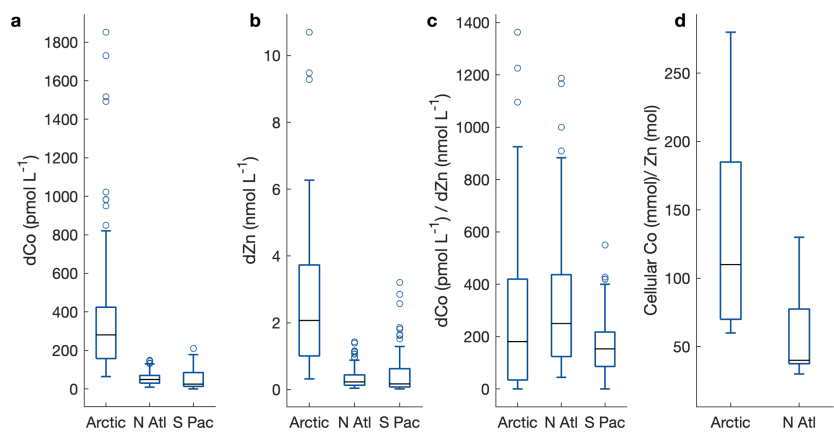


1152 **Figure 14.**



1153 **Figure 15.**





1155 **References**

- 1156 Aagaard, K. and Carmack, E. C.: The role of sea ice and other fresh water in the Arctic
1157 circulation, *J. Geophys. Res. Ocean.*, 94(C10), 14485–14498, 1989.
- 1158 Aumont, O., Van Hulten, M., Roy-Barman, M., Dutay, J.-C., Éthé, C. and Gehlen, M.: Variable
1159 reactivity of particulate organic matter in a global ocean biogeochemical model, 2017.
- 1160 Baars, O. and Croot, P. L.: Dissolved cobalt speciation and reactivity in the eastern tropical
1161 North Atlantic, *Mar. Chem.*, 173, 310–319, doi:10.1016/j.marchem.2014.10.006, 2015.
- 1162 Bauch, D., Erlenkeuser, H. and Andersen, N.: Water mass processes on Arctic shelves as
1163 revealed from $\delta^{18}\text{O}$ of H_2O , *Glob. Planet. Change*, 48(1–3), 165–174, 2005.
- 1164 Bertrand, E. M., Saito, M. A., Rose, J. M., Riesselman, C. R., Lohan, M. C., Noble, A. E., Lee,
1165 P. A. and DiTullio, G. R.: Vitamin B_{12} and iron colimitation of phytoplankton growth in the
1166 Ross Sea, *Limnol. Oceanogr.*, 52(3), 1079–1093, doi:10.4319/lo.2007.52.3.1079, 2007.
- 1167 Bertrand, E. M., Allen, A. E., Dupont, C. L., Norden-Krichmar, T. M., Bai, J., Valas, R. E. and
1168 Saito, M. A.: Influence of cobalamin scarcity on diatom molecular physiology and identification
1169 of a cobalamin acquisition protein, *Proc. Natl. Acad. Sci.*, 109(26), E1762–E1771,
1170 doi:10.1073/pnas.1201731109, 2012.
- 1171 Bertrand, E. M., McCrow, J. P., Moustafa, A., Zheng, H., McQuaid, J. B., Delmont, T. O., Post,
1172 A. F., Sipler, R. E., Spackeen, J. L. and Xu, K.: Phytoplankton–bacterial interactions mediate
1173 micronutrient colimitation at the coastal Antarctic sea ice edge, *Proc. Natl. Acad. Sci.*, 112(32),
1174 9938–9943, 2015.
- 1175 Bown, J., Boye, M., Baker, A., Duvieilbourg, E., Lacan, F., Le Moigne, F., Planchon, F., Speich,
1176 S. and Nelson, D. M.: The biogeochemical cycle of dissolved cobalt in the Atlantic and the
1177 Southern Ocean south off the coast of South Africa, *Mar. Chem.*, 126(1–4), 193–206, 2011.
- 1178 Le Bras, I. A., Yashayaev, I. and Toole, J. M.: Tracking Labrador Sea water property signals
1179 along the deep western boundary current, *J. Geophys. Res. Ocean.*, 122(7), 5348–5366, 2017.
- 1180 Browning, T. J., Achterberg, E. P., Rapp, I., Engel, A., Bertrand, E. M., Tagliabue, A. and
1181 Moore, C. M.: Nutrient co-limitation at the boundary of an oceanic gyre, *Nature*, 551(7679),
1182 242–246, doi:10.1038/nature24063, 2017.
- 1183 Bundy, R. M., Abdulla, H. A. N. N., Hatcher, P. G., Biller, D. V., Buck, K. N. and Barbeau, K.
1184 A.: Iron-binding ligands and humic substances in the San Francisco Bay estuary and estuarine-
1185 influenced shelf regions of coastal California, *Mar. Chem.*, 173, 183–194,
1186 doi:10.1016/j.marchem.2014.11.005, 2015.
- 1187 Carmack, E. C., Macdonald, R. W., Perkin, R. G., McLaughlin, F. A. and Pearson, R. J.:
1188 Evidence for warming of Atlantic water in the southern Canadian Basin of the Arctic Ocean:
1189 Results from the Larsen-93 expedition, *Geophys. Res. Lett.*, 22(9), 1061–1064, 1995.
- 1190 Charette, M. A., Kipp, L. E., Jensen, L. T., Dabrowski, J. S., Whitmore, L. M., Fitzsimmons, J.
1191 N., Williford, T., Ulfssbo, A., Jones, E., Bundy, R. M. and others: The Transpolar Drift as a
1192 Source of Riverine and Shelf-Derived Trace Elements to the Central Arctic Ocean, *J. Geophys.*
1193 *Res. Ocean.*, 2020.
- 1194 Cooper, L. W., Whitley, T. E., Grebmeier, J. M. and Weingartner, T.: The nutrient, salinity,
1195 and stable oxygen isotope composition of Bering and Chukchi Seas waters in and near the
1196 Bering Strait, *J. Geophys. Res. Ocean.*, 102(C6), 12563–12573, 1997.
- 1197 Cooper, L. W., Benner, R., McClelland, J. W., Peterson, B. J., Holmes, R. M., Raymond, P. A.,
1198 Hansell, D. A., Grebmeier, J. M. and Codispoti, L. A.: Linkages among runoff, dissolved organic
1199 carbon, and the stable oxygen isotope composition of seawater and other water mass indicators
1200 in the Arctic Ocean, *J. Geophys. Res. Biogeosciences*, 110(G2), 2005.

1201 Cottrell, M. T. and Kirchman, D. L.: Photoheterotrophic microbes in the Arctic Ocean in summer
 1202 and winter, *Appl. Environ. Microbiol.*, 75(15), 4958–4966, 2009.
 1203 Cowen, J. P. and Bruland, K. W.: Metal deposits associated with bacteria: implications for Fe
 1204 and Mn marine biogeochemistry, *Deep Sea Res. Part A. Oceanogr. Res. Pap.*, 32(3), 253–272,
 1205 1985.
 1206 Cutter, G. A. and Bruland, K. W.: Rapid and noncontaminating sampling system for trace
 1207 elements in global ocean surveys, *Limnol. Oceanogr. Methods*, 10(JUNE), 425–436,
 1208 doi:10.4319/lom.2012.10.425, 2012.
 1209 Doxaran, D., Devred, E. and Babin, M.: A 50% increase in the mass of terrestrial particles
 1210 delivered by the Mackenzie River into the Beaufort Sea (Canadian Arctic Ocean) over the last 10
 1211 years, 2015.
 1212 Doxey, A. C., Kurtz, D. A., Lynch, M. D. J., Sauder, L. A. and Neufeld, J. D.: Aquatic
 1213 metagenomes implicate Thaumarchaeota in global cobalamin production, *ISME J.*, 9(2), 461,
 1214 2015.
 1215 Drake, T. W., Tank, S. E., Zhulidov, A. V., Holmes, R. M., Gurtovaya, T. and Spencer, R. G. M.:
 1216 Increasing alkalinity export from large Russian Arctic rivers, *Environ. Sci. Technol.*, 52(15),
 1217 8302–8308, 2018.
 1218 Dulaquais, G., Boye, M., Middag, R., Owens, S., Puigcorb , V., Buesseler, K. O., Masqu , P., de
 1219 Baar, H. J. W. and Carton, X.: Contrasting biochemical cycles of cobalt in the surface western
 1220 Atlantic ocean, *Global Biogeochem. Cycles*, 28, 1387–1412,
 1221 doi:10.1002/2014GB004903.Received, 2014a.
 1222 Dulaquais, G., Boye, M., Rijkenberg, M. J. A. and Carton, X.: Physical and remineralization
 1223 processes govern the cobalt distribution in the deep western Atlantic Ocean, *Biogeosciences*,
 1224 11(6), 1561–1580, doi:10.5194/bg-11-1561-2014, 2014b.
 1225 Dulaquais, G., Planquette, H., L’Helguen, S., Rijkenberg, M. J. A. and Boye, M.: The
 1226 biogeochemistry of cobalt in the Mediterranean Sea, *Global Biogeochem. Cycles*, 31(2), 377–
 1227 399, doi:10.1002/2016GB005478, 2017.
 1228 Gascard, J., Festy, J., le Goff, H., Weber, M., Bruemmer, B., Offermann, M., Doble, M.,
 1229 Wadhams, P., Forsberg, R. and Hanson, S.: Exploring Arctic transpolar drift during dramatic sea
 1230 ice retreat, *Eos, Trans. Am. Geophys. Union*, 89(3), 21–22, 2008.
 1231 Hawco, N. J. and Saito, M. A.: Competitive inhibition of cobalt uptake by zinc and manganese in
 1232 a pacific *Prochlorococcus* strain: Insights into metal homeostasis in a streamlined oligotrophic
 1233 cyanobacterium, *Limnol. Oceanogr.*, 63(5), 2229–2249, 2018.
 1234 Hawco, N. J., Ohnemus, D. C., Resing, J. A., Twining, B. S. and Saito, M. A.: A dissolved cobalt
 1235 plume in the oxygen minimum zone of the eastern tropical South Pacific, *Biogeosciences*,
 1236 13(20), 5697–5717, doi:10.5194/bg-13-5697-2016, 2016.
 1237 Hawco, N. J., Lam, P. J., Lee, J. M., Ohnemus, D. C., Noble, A. E., Wyatt, N. J., Lohan, M. C.
 1238 and Saito, M. A.: Cobalt scavenging in the mesopelagic ocean and its influence on global mass
 1239 balance: Synthesizing water column and sedimentary fluxes, *Mar. Chem.*, 201(March 2017),
 1240 151–166, doi:10.1016/j.marchem.2017.09.001, 2018.
 1241 Hawco, N. J., McIlvin, M. M., Bundy, R. M., Tagliabue, A., Goepfert, T. J., Moran, D. M.,
 1242 Valentin-Alvarado, L., DiTullio, G. R. and Saito, M. A.: Minimal cobalt metabolism in the
 1243 marine cyanobacterium *Prochlorococcus*, *Proc. Natl. Acad. Sci.*, 2020.
 1244 Heal, K.: The Power and Promise of Direct Measurements of Metabolites in Marine Systems,
 1245 2018.
 1246 Heal, K. R., Qin, W., Ribalet, F., Bertagnolli, A. D., Coyote-Maestas, W., Hmelo, L. R., Moffett,

1247 J. W., Devol, A. H., Armbrust, E. V. and Stahl, D. A.: Two distinct pools of B12 analogs reveal
 1248 community interdependencies in the ocean, *Proc. Natl. Acad. Sci.*, 114(2), 364–369, 2017.
 1249 Holmes, R. M., McClelland, J. W., Tank, S. E., Spencer, R. G. . and Shiklomanov, A. I.: Arctic
 1250 Great Rivers Observatory Water Quality Dataset. [online] Available from:
 1251 <https://www.arcticgreatrivers.org/data>, 2018.
 1252 Jensen, L., Wyatt, N., Twining, B., Rauschenberg, S., Landing, W., Sherrell, R. and
 1253 Fitzsimmons, J.: Biogeochemical cycling of dissolved zinc in the Western Arctic (Arctic
 1254 GEOTRACES GN01), *Global Biogeochem. Cycles*, 33(3), 343–369, 2019.
 1255 Johannessen, O. M., Bengtsson, L., Miles, M. W., Kuzmina, S. I., Semenov, V. A., Alekseev, G.
 1256 V., Nagurnyi, A. P., Zakharov, V. F., Bobylev, L. P. and Pettersson, L. H.: Arctic climate change:
 1257 observed and modelled temperature and sea-ice variability, *Tellus A Dyn. Meteorol. Oceanogr.*,
 1258 56(4), 328–341, 2004.
 1259 Johnson, K. S., Berelson, W. M., Coale, K. H., Coley, T. L., Elrod, V. A., Fairey, W. R., Iams,
 1260 H. D., Kilgore, T. E. and Nowicki, J. L.: Mangense flux from continental-margin sediments in a
 1261 transect through the oxygen minimum, *Science* (80-.), 257(5074), 1242–1245,
 1262 doi:10.1126/science.257.5074.1242, 1992.
 1263 Jorgenson, M. T., Shur, Y. L. and Pullman, E. R.: Abrupt increase in permafrost degradation in
 1264 Arctic Alaska, *Geophys. Res. Lett.*, 33(2), 2006.
 1265 Kipp, L. E., Charette, M. A., Moore, W. S., Henderson, P. B. and Rigor, I. G.: Increased fluxes
 1266 of shelf-derived materials to the central Arctic Ocean, *Sci. Adv.*, 4(1), eaao1302, 2018.
 1267 Klunder, M. B., Bauch, D., Laan, P., de Baar, H. J. W., van Heuven, S. and Ober, S.: Dissolved
 1268 iron in the Arctic shelf seas and surface waters of the central Arctic Ocean: Impact of Arctic
 1269 river water and ice-melt, *J. Geophys. Res.*, 117, 18, doi:C01027 10.1029/2011jc007133, 2012.
 1270 Lane, T. W. and Morel, F. M. M.: Regulation of carbonic anhydrase expression by zinc, cobalt,
 1271 and carbon dioxide in the marine diatom *Thalassiosira weissflogii*, *Plant Physiol.*, 123(1), 345–
 1272 352, 2000.
 1273 Lee, J.-M., Heller, M. I. and Lam, P. J.: Size distribution of particulate trace elements in the US
 1274 GEOTRACES Eastern Pacific Zonal Transect (GP16), *Mar. Chem.*, 201, 108–123, 2018.
 1275 Lionheart, R.: Exploring the ocean microbiome: quantified cobalamin production in pelagic
 1276 bacteria using liquid chromatography and mass spectrometry, 2017.
 1277 van der Loeff, M., Kipp, L., Charette, M. A., Moore, W. S., Black, E., Stimac, I., Charkin, A.,
 1278 Bauch, D., Valk, O., Karcher, M. and others: Radium isotopes across the Arctic Ocean show
 1279 time scales of water mass ventilation and increasing shelf inputs, *J. Geophys. Res. Ocean.*,
 1280 123(7), 4853–4873, 2018.
 1281 Marsay, C. M., Aguilar-Islas, A., Fitzsimmons, J. N., Hatta, M., Jensen, L. T., John, S. G.,
 1282 Kadko, D., Landing, W. M., Lanning, N. T., Morton, P. L., Pasqualini, A., Rauschenberg, S.,
 1283 Sherrell, R. M., Shiller, A. M., Twining, B. S., Whitmore, L. M., Zhang, R., Buck, C. S. and
 1284 others: Dissolved and particulate trace elements in late summer Arctic melt ponds, *Mar. Chem.*,
 1285 204(June), 70–85, doi:10.1016/j.marchem.2018.06.002, 2018.
 1286 Martin, J. H., Gordon, R. M., Fitzwater, S. and Broenkow, W. W.: VERTEX: phytoplankton/iron
 1287 studies in the Gulf of Alaska, *Deep Sea Res. Part A. Oceanogr. Res. Pap.*, 36(5), 649–680, 1989.
 1288 März, C., Stratmann, A., Matthiessen, J., Meinhardt, A. K., Eckert, S., Schnetger, B., Vogt, C.,
 1289 Stein, R. and Brumsack, H. J.: Manganese-rich brown layers in Arctic Ocean sediments:
 1290 Composition, formation mechanisms, and diagenetic overprint, *Geochim. Cosmochim. Acta*,
 1291 75(23), 7668–7687, doi:10.1016/j.gca.2011.09.046, 2011.
 1292 McManus, J., Berelson, W. M., Severmann, S., Johnson, K. S., Hammond, D. E., Roy, M. and

1293 Coale, K. H.: Benthic manganese fluxes along the Oregon-California continental shelf and slope,
 1294 *Cont. Shelf Res.*, 43, 71–85, doi:10.1016/j.csr.2012.04.016, 2012.
 1295 Middag, R., De Baar, H. J. W., Laan, P. and Klunder, M. B.: Fluvial and hydrothermal input of
 1296 manganese into the Arctic Ocean, *Geochim. Cosmochim. Acta*, 75(9), 2393–2408, 2011.
 1297 Moffett, J. W. and Ho, J.: Oxidation of cobalt and manganese in seawater via a common
 1298 microbially catalyzed pathway, *Geochim. Cosmochim. Acta*, 60(18), 3415–3424,
 1299 doi:10.1016/0016-7037(96)00176-7, 1996.
 1300 Moore, C. M., Mills, M. M., Arrigo, K. R., Berman-Frank, I., Bopp, L., Boyd, P. W., Galbraith,
 1301 E. D., Geider, R. J., Guieu, C., Jaccard, S. L., Jickells, T. D., La Roche, J., Lenton, T. M.,
 1302 Mahowald, N. M., Marañón, E., Marinov, I., Moore, J. K., Nakatsuka, T., Oschlies, A., Saito, M.
 1303 A., Thingstad, T. F., Tsuda, A., Ulloa, O., Maranon, E., Marinov, I., Moore, J. K., Nakatsuka, T.,
 1304 Oschlies, A., Saito, M. A., Thingstad, T. F., Tsuda, A. and Ulloa, O.: Processes and patterns of
 1305 oceanic nutrient limitation, *Nat. Geosci.*, 6(9), 701–710, doi:10.1038/ngeo1765, 2013.
 1306 Newton, R., Schlosser, P., Mortlock, R., Swift, J. and MacDonald, R.: Canadian Basin
 1307 freshwater sources and changes: Results from the 2005 Arctic Ocean Section, *J. Geophys. Res.*
 1308 *Ocean.*, 118(4), 2133–2154, 2013.
 1309 Noble, A. E.: Influences on the oceanic biogeochemical cycling of the hybrid-type metals,
 1310 cobalt, iron, and manganese, Massachusetts Institute of Technology., 2012.
 1311 Noble, A. E., Saito, M. A., Maiti, K. and Benitez-Nelson, C. R.: Cobalt, manganese, and iron
 1312 near the Hawaiian Islands: A potential concentrating mechanism for cobalt within a cyclonic
 1313 eddy and implications for the hybrid-type trace metals, *Deep Sea Res. Part II Top. Stud.*
 1314 *Oceanogr.*, 55(10–13), 1473–1490, 2008.
 1315 Noble, A. E., Lamborg, C. H., Ohnemus, D. C., Lam, P. J., Goepfert, T. J., Measures, C. I.,
 1316 Frame, C. H., Casciotti, K. L., DiTullio, G. R., Jennings, J. and Saito, M. A.: Basin-scale inputs
 1317 of cobalt, iron, and manganese from the Benguela-Angola front to the South Atlantic Ocean,
 1318 *Limnol. Oceanogr.*, 57(4), 989–1010, doi:10.4319/lo.2012.57.4.0989, 2012.
 1319 Noble, A. E., Ohnemus, D. C., Hawco, N. J., Lam, P. J. and Saito, M. A.: Coastal sources, sinks
 1320 and strong organic complexation of dissolved cobalt within the US North Atlantic GEOTRACES
 1321 transect GA03, *Biogeosciences*, 14(11), 2715–2739, doi:10.5194/bg-14-2715-2017, 2016.
 1322 Panzeca, C., Beck, A. J., Leblanc, K., Taylor, G. T., Hutchins, D. A. and Sanudo-Wilhelmy, S.
 1323 A.: Potential cobalt limitation of vitamin B12 synthesis in the North Atlantic Ocean, *Global*
 1324 *Biogeochem. Cycles*, 22(2), 2008.
 1325 Resing, J. A. and Mottl, M. J.: Determination of manganese in seawater using flow injection
 1326 analysis with on-line preconcentration and spectrophotometric detection, *Anal. Chem.*, 64(22),
 1327 2682–2687, 1992.
 1328 Saito, M. A. and Moffett, J. W.: Complexation of cobalt by natural organic ligands in the
 1329 Sargasso Sea as determined by a new high-sensitivity electrochemical cobalt speciation method
 1330 suitable for open ocean work, *Mar. Chem.*, 75(1–2), 49–68, doi:10.1016/s0304-4203(01)00025-
 1331 1, 2001a.
 1332 Saito, M. A. and Moffett, J. W.: Complexation of cobalt by natural organic ligands in the
 1333 Sargasso Sea as determined by a new high-sensitivity electrochemical cobalt speciation method
 1334 suitable for open ocean work, *Mar. Chem.*, 75(1–2), 49–68, doi:10.1016/s0304-4203(01)00025-
 1335 1, 2001b.
 1336 Saito, M. A., Moffett, J. W., Chisholm, S. W. and Waterbury, J. B.: Cobalt limitation and uptake
 1337 in *Prochlorococcus*, *Limnol. Oceanogr.*, 47(6), 1629–1636, 2002.
 1338 Saito, M. A., Moffett, J. W. and DiTullio, G. R.: Cobalt and nickel in the Peru upwelling region:

1339 A major flux of labile cobalt utilized as a micronutrient, *Global Biogeochem. Cycles*, 18(4), 1–
 1340 14, doi:10.1029/2003GB002216, 2004.
 1341 Saito, M. A., Rocap, G. and Moffett, J. W.: Production of cobalt binding ligands in a
 1342 *Synechococcus* feature at the Costa Rica upwelling dome, *Limnol. Oceanogr.*, 50(1), 279–290,
 1343 2005.
 1344 Saito, M. A., Goepfert, T. J., Noble, A. E., Bertrand, E. M., Sedwick, P. N. and DiTullio, G. R.:
 1345 A seasonal study of dissolved cobalt in the Ross Sea, Antarctica: micronutrient behavior,
 1346 absence of scavenging, and relationships with Zn, Cd, and P, *Biogeosciences*, 7(12), 4059–4082,
 1347 doi:10.5194/bg-7-4059-2010, 2010.
 1348 Saito, M. A., Noble, A. E., Hawco, N., Twining, B. S., Ohnemus, D. C., John, S. G., Lam, P.,
 1349 Conway, T. M., Johnson, R., Moran, D. and McIlvin, M.: The acceleration of dissolved cobalt's
 1350 ecological stoichiometry due to biological uptake, remineralization, and scavenging in the
 1351 Atlantic Ocean, *Biogeosciences*, 14(20), 4637–4662, doi:10.5194/bg-14-4637-2017, 2017.
 1352 Screen, J. A. and Simmonds, I.: The central role of diminishing sea ice in recent Arctic
 1353 temperature amplification, *Nature*, 464(7293), 1334, 2010.
 1354 Serreze, M. C. and Barry, R. G.: Processes and impacts of Arctic amplification: A research
 1355 synthesis, *Glob. Planet. Change*, 77(1–2), 85–96, 2011.
 1356 Shelley, R. U., Sedwick, P. N., Bibby, T. S., Cabedo-Sanz, P., Church, T. M., Johnson, R. J.,
 1357 Macey, A. I., Marsay, C. M., Sholkovitz, E. R. and Ussher, S. J.: Controls on dissolved cobalt in
 1358 surface waters of the Sargasso Sea: Comparisons with iron and aluminum, *Global Biogeochem.*
 1359 *Cycles*, 26(2), 2012.
 1360 Steele, M. and Boyd, T.: Retreat of the cold halocline layer in the Arctic Ocean, *J. Geophys. Res.*
 1361 *Ocean.*, 103(C5), 10419–10435, 1998.
 1362 Steele, M., Morison, J., Ermold, W., Rigor, I., Ortmeyer, M. and Shimada, K.: Circulation of
 1363 summer Pacific halocline water in the Arctic Ocean, *J. Geophys. Res. Ocean.*, 109(C2), 2004.
 1364 Stroeve, J. C., Serreze, M. C., Holland, M. M., Kay, J. E., Malanik, J. and Barrett, A. P.: The
 1365 Arctic's rapidly shrinking sea ice cover: a research synthesis, *Clim. Change*, 110(3–4), 1005–
 1366 1027, 2012.
 1367 Sunda, W. G. and Huntsman, S. A.: Effect of sunlight on redox cycles of manganese in the
 1368 southwestern Sargasso Sea, *Deep Sea Res. Part A. Oceanogr. Res. Pap.*, 35(8), 1297–1317, 1988.
 1369 Sunda, W. G. and Huntsman, S. A.: Cobalt and zinc interreplacement in marine phytoplankton:
 1370 biological and geochemical implications, *Limnol. Oceanogr.*, 40(8), 1404–1417, 1995.
 1371 Swift, J. H., Takahashi, T. and Livingston, H. D.: The contribution of the Greenland and Barents
 1372 seas to the deep water of the Arctic Ocean, *J. Geophys. Res. Ocean.*, 88(C10), 5981–5986, 1983.
 1373 Tagliabue, A., Hawco, N. J., Bundy, R. M., Landing, W. M., Milne, A., Morton, P. L. and Saito,
 1374 M. A.: The role of external inputs and internal cycling in shaping the global ocean cobalt
 1375 distribution: insights from the first cobalt biogeochemical model, *Global Biogeochem. Cycles*,
 1376 32(4), 1–23, doi:10.1002/2017GB005830, 2018.
 1377 Tank, S. E., Striegl, R. G., McClelland, J. W. and Kokelj, S. V: Multi-decadal increases in
 1378 dissolved organic carbon and alkalinity flux from the Mackenzie drainage basin to the Arctic
 1379 Ocean, *Environ. Res. Lett.*, 11(5), 54015, 2016.
 1380 Tebo, B. M., Bargar, J. R., Clement, B. G., Dick, G. J., Murray, K. J., Parker, D., Verity, R. and
 1381 Webb, S. M.: Biogenic manganese oxides: properties and mechanisms of formation, *Annu. Rev.*
 1382 *Earth Planet. Sci.*, 32, 287–328, 2004.
 1383 Thuróczy, C. E., Boye, M. and Losno, R.: Dissolution of cobalt and zinc from natural and
 1384 anthropogenic dusts in seawater, *Biogeosciences*, 7, 1927–1936, 2010.

1385 Tonnard, M., Planquette, H., Bowie, A., Van Der Merwe, P., Gallinari, M., de Gésincourt, F. D.,
 1386 Germain, Y., Gourain, A., Benetti, M., Reverdin, G. and others: Dissolved iron in the North
 1387 Atlantic Ocean and Labrador Sea along the GEOVIDE section (GEOTRACES section GA01),
 1388 Biogeosciences, 17(4), 917–943, 2020.
 1389 Toohey, R. C., Herman-Mercer, N. M., Schuster, P. F., Mutter, E. A. and Koch, J. C.:
 1390 Multidecadal increases in the Yukon River Basin of chemical fluxes as indicators of changing
 1391 flowpaths, groundwater, and permafrost, Geophys. Res. Lett., 43(23), 12–120, 2016.
 1392 Tovar-Sánchez, A., Sañudo-Wilhelmy, S. A. and Flegal, A. R.: Temporal and spatial variations
 1393 in the biogeochemical cycling of cobalt in two urban estuaries: Hudson River Estuary and San
 1394 Francisco Bay, Estuar. Coast. Shelf Sci., 60(4), 717–728, 2004.
 1395 Twining, B. S., Rauschenberg, S., Morton, P. L., Ohnemus, D. C. and Lam, P. J.: Comparison of
 1396 particulate trace element concentrations in the North Atlantic Ocean as determined with discrete
 1397 bottle sampling and in situ pumping, Deep. Res. Part II Top. Stud. Oceanogr., 116, 273–282,
 1398 doi:10.1016/j.dsr2.2014.11.005, 2015.
 1399 Twining, B. S., Morton, P. L. and Salters, V. J.: Trace element concentrations (labile and total
 1400 measurements) in particles collected with GO-Flo bottles and analyzed with ICP-MS from the
 1401 US GEOTRACES Arctic cruise (HLY1502; GNo1) from August to October 2015., Biol. Chem.
 1402 Oceanogr. Data Manag. Off., (2019-07–02), doi:10.1575/1912/bco-dmo.771474.2, 2019.
 1403 Del Vecchio, R. and Blough, N. V.: On the origin of the optical properties of humic substances,
 1404 Environ. Sci. Technol., 38(14), 3885–3891, 2004.
 1405 Waleron, M., Waleron, K., Vincent, W. F. and Wilmotte, A.: Allochthonous inputs of riverine
 1406 picocyanobacteria to coastal waters in the Arctic Ocean, FEMS Microbiol. Ecol., 59(2), 356–
 1407 365, 2007.
 1408 Wheeler, P. A., Watkins, J. M. and Hansing, R. L.: Nutrients, organic carbon and organic
 1409 nitrogen in the upper water column of the Arctic Ocean: implications for the sources of dissolved
 1410 organic carbon, Deep Sea Res. Part II Top. Stud. Oceanogr., 44(8), 1571–1592, 1997.
 1411 Yang, R. J. and Van Den Berg, C. M. G.: Metal Complexation by Humic Substances in
 1412 Seawater, Environ. Sci. Technol., 43(19), 7192–7197, doi:10.1021/es900173w, 2009.
 1413 Yee, D. and Morel, F. M. M.: In vivo substitution of zinc by cobalt in carbonic anhydrase of a
 1414 marine diatom, Limnol. Oceanogr., 41(3), 573–577, 1996.
 1415 Zakhia, F., Jungblut, A.-D., Taton, A., Vincent, W. F. and Wilmotte, A.: Cyanobacteria in cold
 1416 ecosystems, in Psychrophiles: from biodiversity to biotechnology, pp. 121–135, Springer., 2008.
 1417 Zhang, H., Van Den Berg, C. M. G. and Wollast, R.: The determination of interactions of cobalt
 1418 (II) with organic compounds in seawater using cathodic stripping voltammetry, Mar. Chem.,
 1419 28(4), 285–300, 1990.
 1420 Zhang, Y., Rodionov, D. A., Gelfand, M. S. and Gladyshev, V. N.: Comparative genomic
 1421 analyses of nickel, cobalt and vitamin B12 utilization, BMC Genomics, 10(1), 78, 2009.
 1422